Supplementary information for: ‘Rapid crustal transit of magma drives magmatic rifting in Ethiopia’

Kevin Wong[1,2,*], Daniel Morgan[1], David Ferguson[1], Marie Edmonds[3], Amdemichael Zafu Tadesse[4,5], Maeve Murphy Quinlan[1], Gezahegn Yirgu[5], and Tim Wright[1]

[1]Centre for the Observation and Modelling of Earthquakes, Volcanoes and Tectonics (COMET), School of Earth and Environment, University of Leeds, Leeds LS2 9JT, United Kingdom
[2]Dipartimento di Scienze Biologiche, Geologiche e Ambientali (BiGeA), Alma Mater Studiorum Università di Bologna, Piazza di Porta San Donato 1, 40126 Bologna, Italy
[3]Centre for the Observation and Modelling of Earthquakes, Volcanoes and Tectonics (COMET), Department of Earth Sciences, University of Cambridge, Cambridge CB2 3EQ, United Kingdom
[4]Department of Earth Sciences, University of Oxford, Oxford OX1 3AN, United Kingdom
[5]School of Earth Sciences, Addis Ababa University, P. O. Box 1176 Addis Ababa, Ethiopia
*corresponding author: kevin.wong@unibo.it

This supplementary file includes the following:

Table S1

Figures S1–S31

References for figure captions

Table S1. Primitive basalt compositions from the Boku Volcanic Complex and East Ziway cone fields used in Petrolog3 (NB-01 and Z67) and RhyoliteMELTS 1.2.0 *(Z58) modelling. Note that Z58 and Z67, both collected from the Ziway cone field, represent the melt in which our olivines are obtained and the most primitive melt sampled within Ziway respectively. Z67 is chosen in lieu of Z58 for Petrolog modelling to allow for a greater range of crystallising olivine Fo.*

Oxide (wt.%)	**Boku (NB-01)**	**Ziway (Z58)**	**Ziway (Z67)**
SiO_2	45.43	47.75	44.98
TiO_2	2.19	2.17	2.19
Al_2O_3	16.81	14.54	13.76
Fe_2O_3	12.74	12.16	12.43
MnO	0.16	0.19	0.20
MgO	8.81	7.39	9.24
CaO	10.52	9.09	10.49
Na_2O	2.52	2.95	2.41
K_2O	0.46	1.04	0.56
P_2O_5	0.33	0.54	0.30
Cr_2O_3	0.00	0.05	0.07
H_2O	1.00	Variable (Fig. S2)	1.00

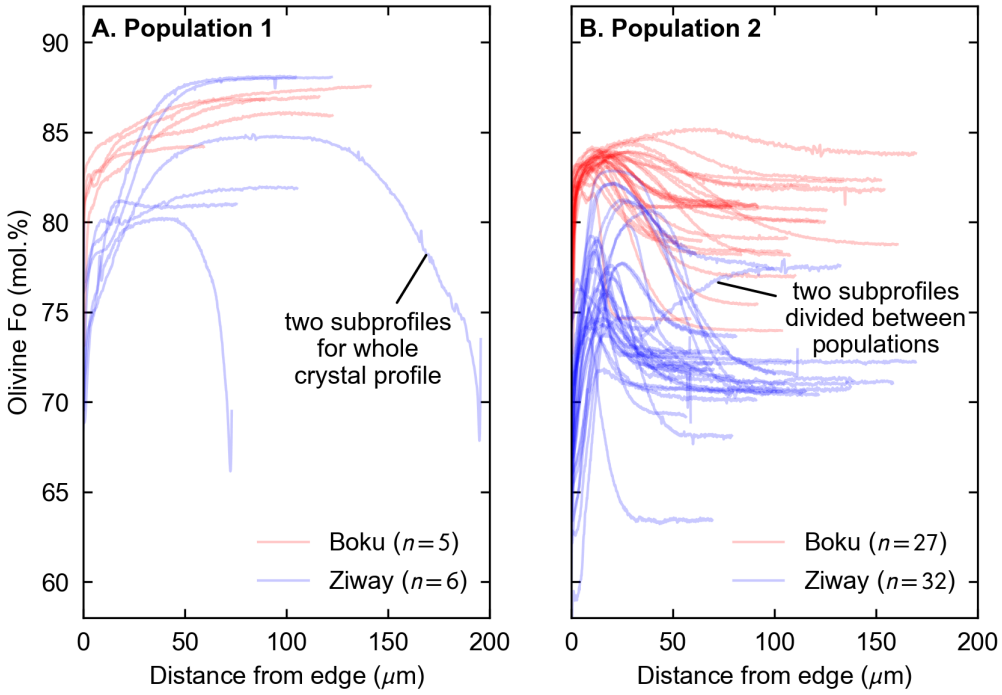

Figure S1. Collated plots of olivine profiles from Boku and Ziway. We highlight two distinct profiles from each population: A. A cross-crystal profile of sample ZB_A5 from Ziway is divided into two subprofiles for Autodiff modelling. B. Sample ZB_D6 possesses a normal-zoned interior and a reverse-zoned exterior. For the purposes of this study, this profile is divided into two sub-profiles which are divided accordingly between the two populations.

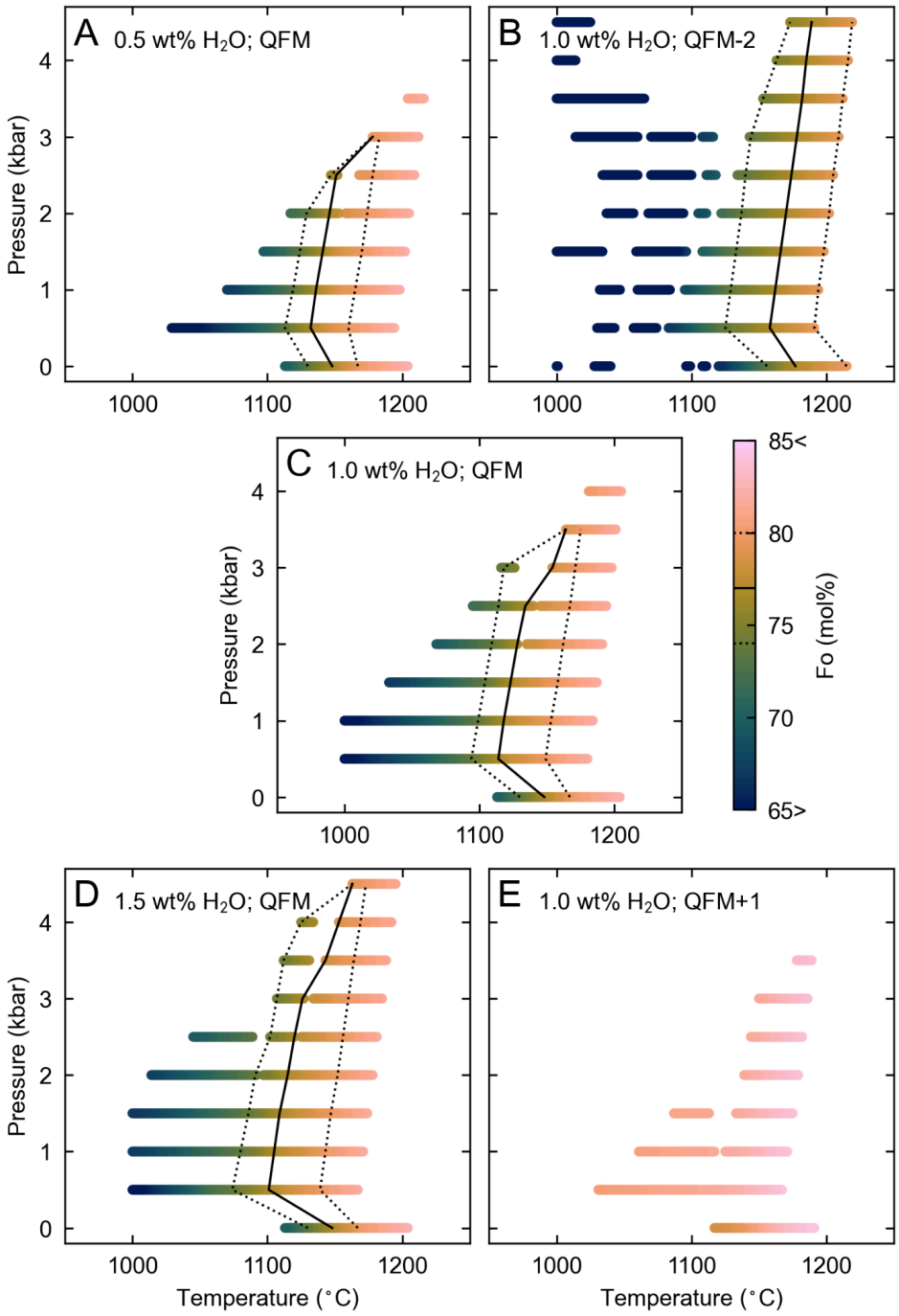
A 0.5 wt% H2O; QFM
B 1.0 wt% H2O; QFM-2
C 1.0 wt% H2O; QFM
D 1.5 wt% H2O; QFM
E 1.0 wt% H2O; QFM+1
Pressure (kbar)
Temperature (°C)
Fo (mol%)
85<
80
75
70
65>
0
1
2
3
4
1000
1100
1200

Figure S2: Rhyolite-MELTS v1.2.0 models [1] for composition Z58 from East Ziway (Table S1). The solid black line marks Fo_{77}, the median rim composition of Ziway reverse-zoned olivines; the dotted black lines mark 1σ of ±3 mol% Fo. Models are run at pressure intervals of 0.5 kbar up to a maximum pressure of 4.5 kbar [2]. Initial melt H_2O contents [2,3] and oxygen fugacity conditions [4,5] for each model are provided as annotations within each subfigure.

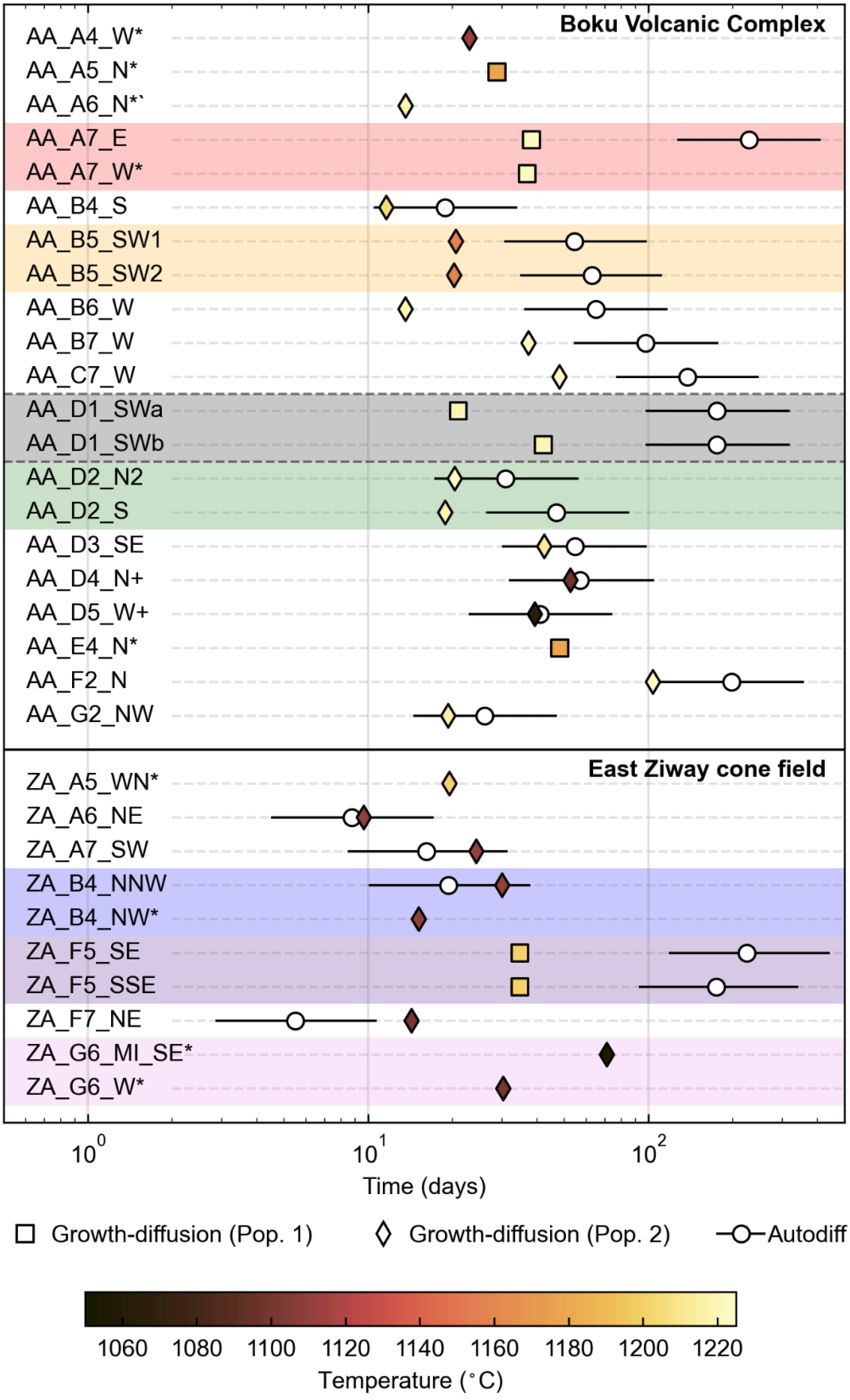
Boku Volcanic Complex
AA_A4_W*
AA_A5_N*
AA_A6_N*`
AA_A7_E
AA_A7_W*
AA_B4_S
AA_B5_SW1
AA_B5_SW2
AA_B6_W
AA_B7_W
AA_C7_W
AA_D1_SWa
AA_D1_SWb
AA_D2_N2
AA_D2_S
AA_D3_SE
AA_D4_N+
AA_D5_W+
AA_E4_N*
AA_F2_N
AA_G2_NW
East Ziway cone field
ZA_A5_WN*
ZA_A6_NE
ZA_A7_SW
ZA_B4_NNW
ZA_B4_NW*
ZA_F5_SE
ZA_F5_SSE
ZA_F7_NE
ZA_G6_MI_SE*
ZA_G6_W*
10^0
10^1
10^2
Time (days)
Growth-diffusion (Pop. 1)
Growth-diffusion (Pop. 2)
Autodiff
1060 1080 1100 1120 1140 1160 1180 1200 1220
Temperature (°C)

Figure S3. All olivine Fe-Mg interdiffusion profile timescales recorded by the growth-diffusion model for both localities. Corresponding Autodiff results with 1σ uncertainties are shown on the same level as each growth-diffusion timescale. Profile labels with an asterisk (*) are growth-diffusion timescales without a corresponding Autodiff timescale; those with a plus symbol (+) have a stepped starting condition (see Supplementary Figures 29). Paired profiles, highlighted with the same background colour, are recorded from the same crystal, and should therefore return self-similar timescales. The paired profiles bracketed by dashed lines (AA_D1_SWa and AA_D1_SWb) are two models with different conditions which match the profile with a similar degree of fitness. Growth-diffusion timescale markers (square for normal-zoned Population 1; diamond for reverse-zoned Population 2), are coloured by the magmatic temperature which best replicates the observed profile shape.

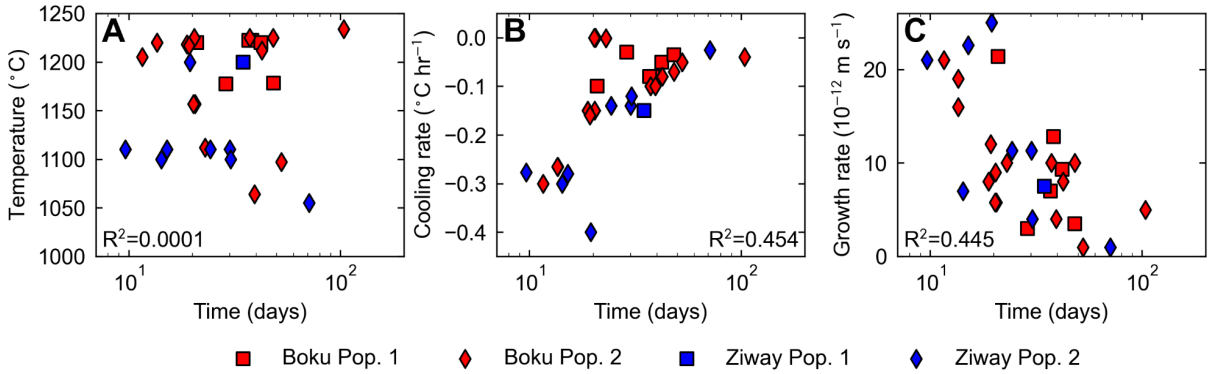

Figure S4: Main Ethiopian Rift olivine timescales from growth-diffusion modelling plotted against growth-diffusion parameters. Population 1 olivines are shown as the square markers; Population 2 olivines are shown as diamonds; Boku and Ziway olivines are red and blue respectively.

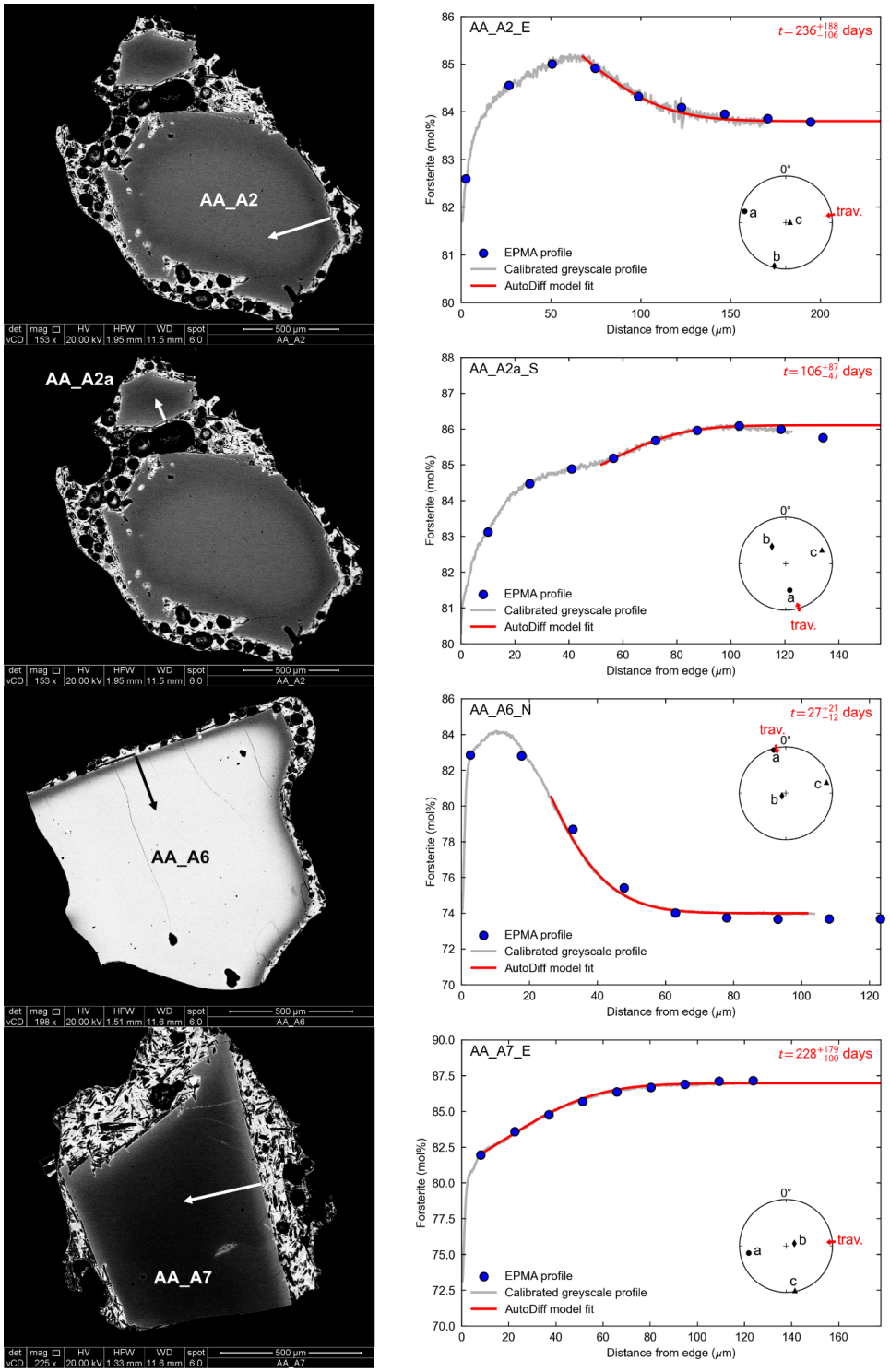

Figures S5–S22: Backscatter electron images showing profile traverses across Main Ethiopian Rift olivines, and plots showing Fo change with traverse distance across profiles. Autodiff model fits are shown as the red line. Pole figures showing crystallographic orientation are shown as inset figures.

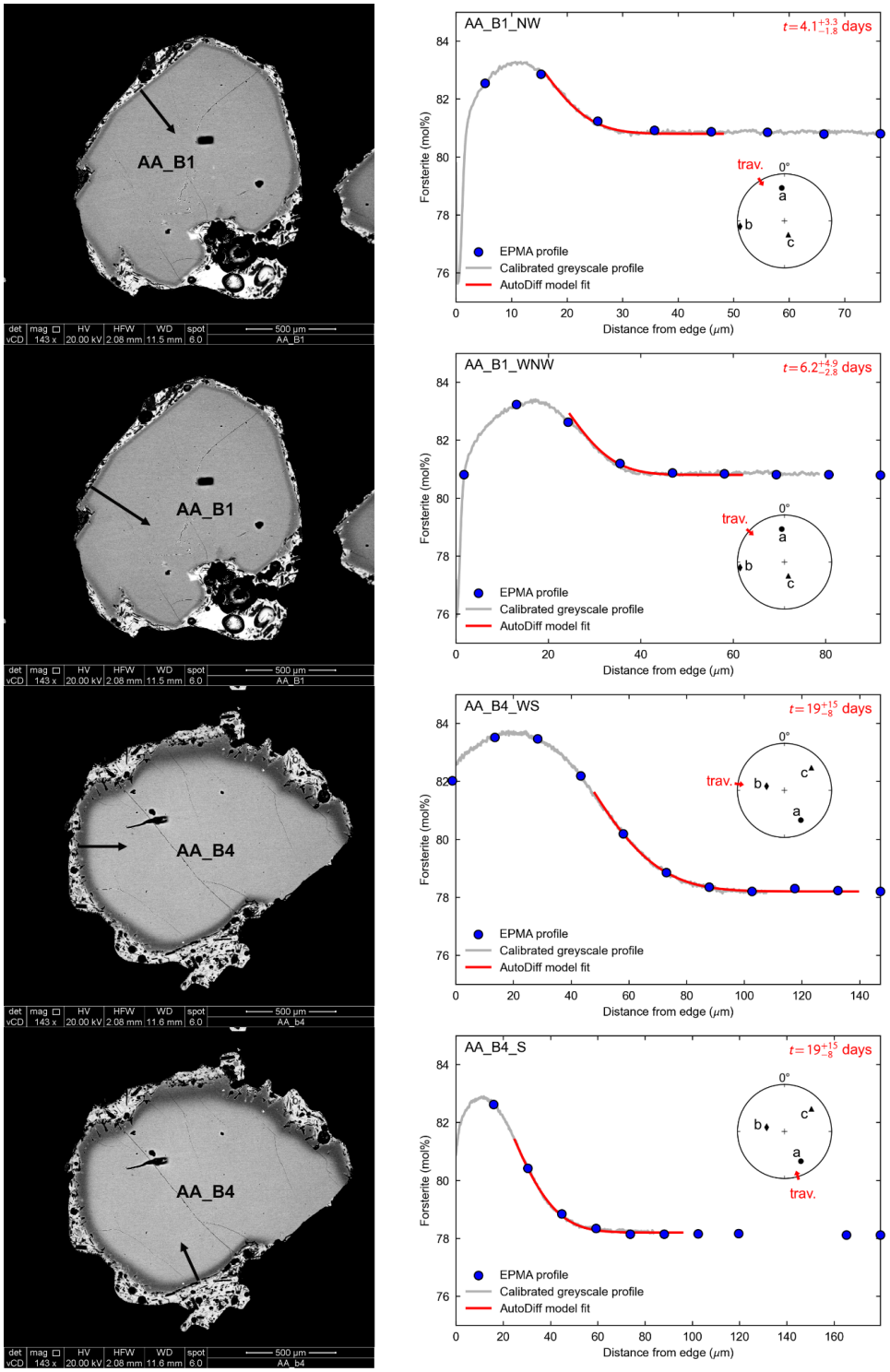
AA_B1
AA_B1
AA_B4
AA_B4
AA_B1_NW
$t = 4.1^{+3.3}_{-1.8}$ days
AA_B1_WNW
$t = 6.2^{+4.9}_{-2.8}$ days
AA_B4_WS
$t = 19^{+15}_{-8}$ days
AA_B4_S
$t = 19^{+15}_{-8}$ days
Forsterite (mol%)
Distance from edge (μm)
EPMA profile
Calibrated greyscale profile
AutoDiff model fit
trav.
0°
a
b
c

Figure S6.

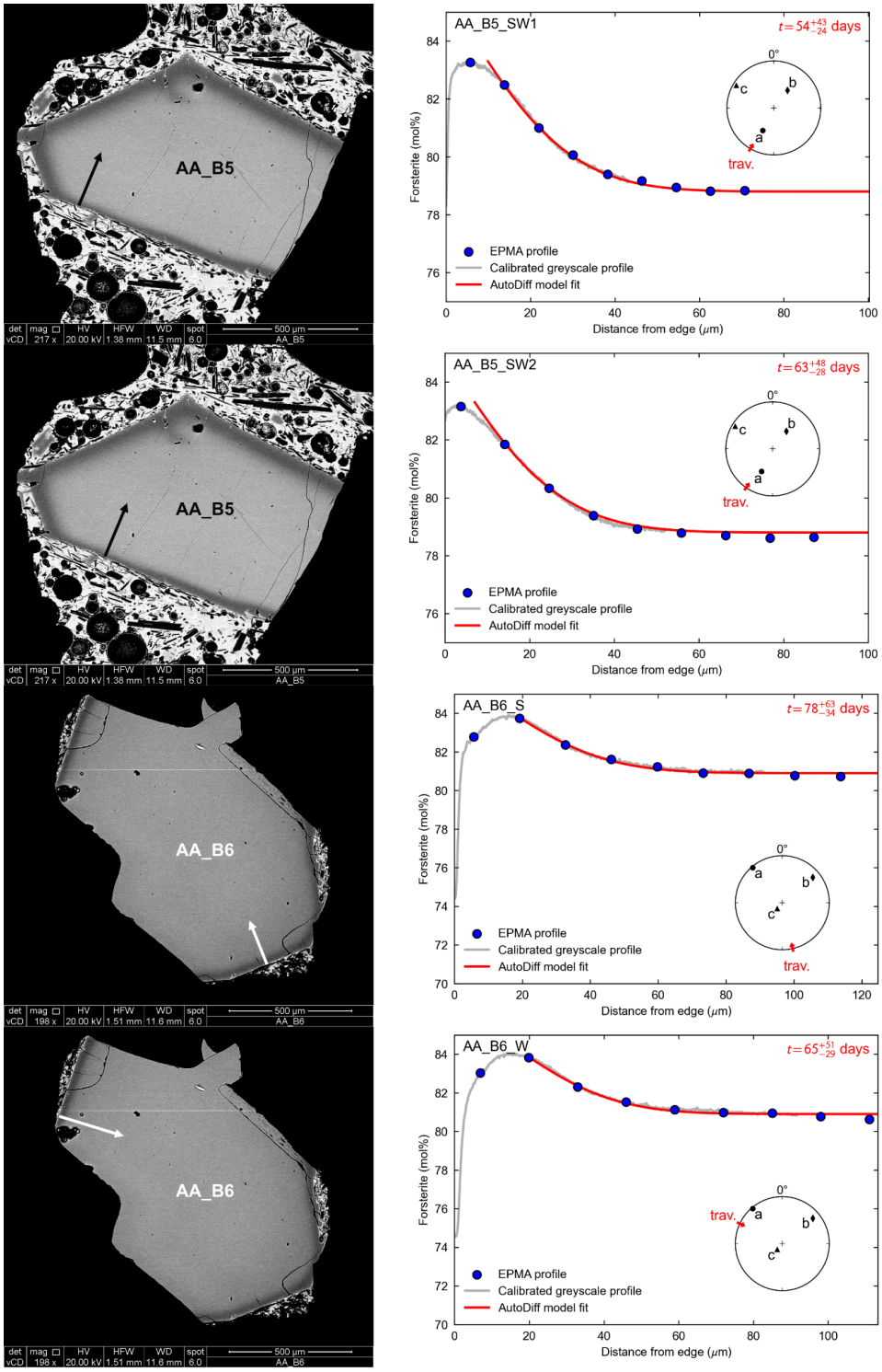
AA_B5
AA_B5
AA_B6
AA_B6
AA_B5_SW1
$t = 54^{+43}_{-24}$ days
AA_B5_SW2
$t = 63^{+48}_{-28}$ days
AA_B6_S
$t = 78^{+63}_{-34}$ days
AA_B6_W
$t = 65^{+51}_{-29}$ days
Forsterite (mol%)
Distance from edge (μm)
EPMA profile
Calibrated greyscale profile
AutoDiff model fit
trav.
0°
a
b
c

Figure S7.

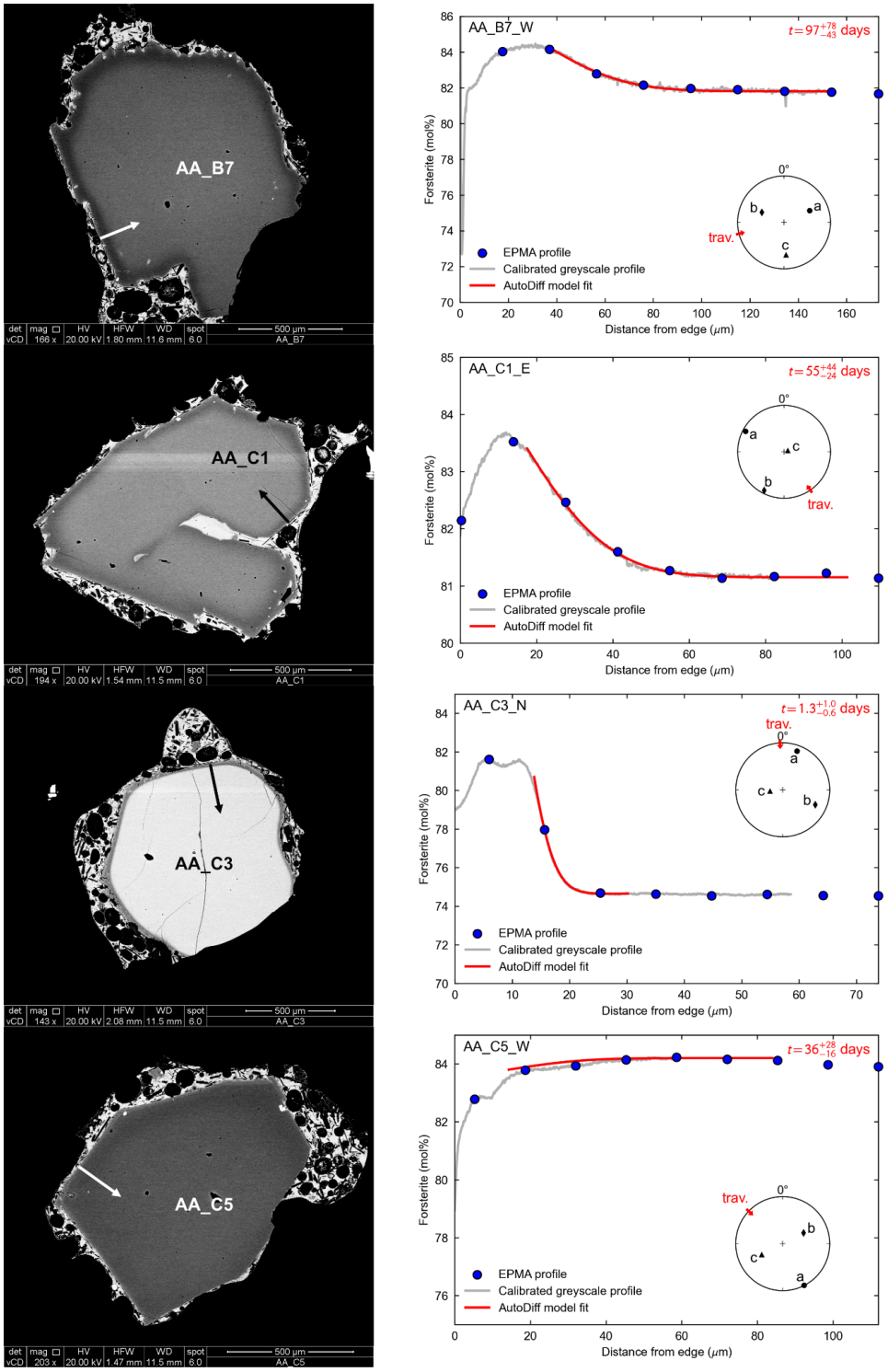
AA_B7
AA_C1
AA_C3
AA_C5
AA_B7_W
$t = 97^{+78}_{-43}$ days
AA_C1_E
$t = 55^{+44}_{-24}$ days
AA_C3_N
$t = 1.3^{+1.0}_{-0.6}$ days
AA_C5_W
$t = 36^{+28}_{-16}$ days
Forsterite (mol%)
Distance from edge (μm)
EPMA profile
Calibrated greyscale profile
AutoDiff model fit
trav.
0°
a
b
c

Figure S8.

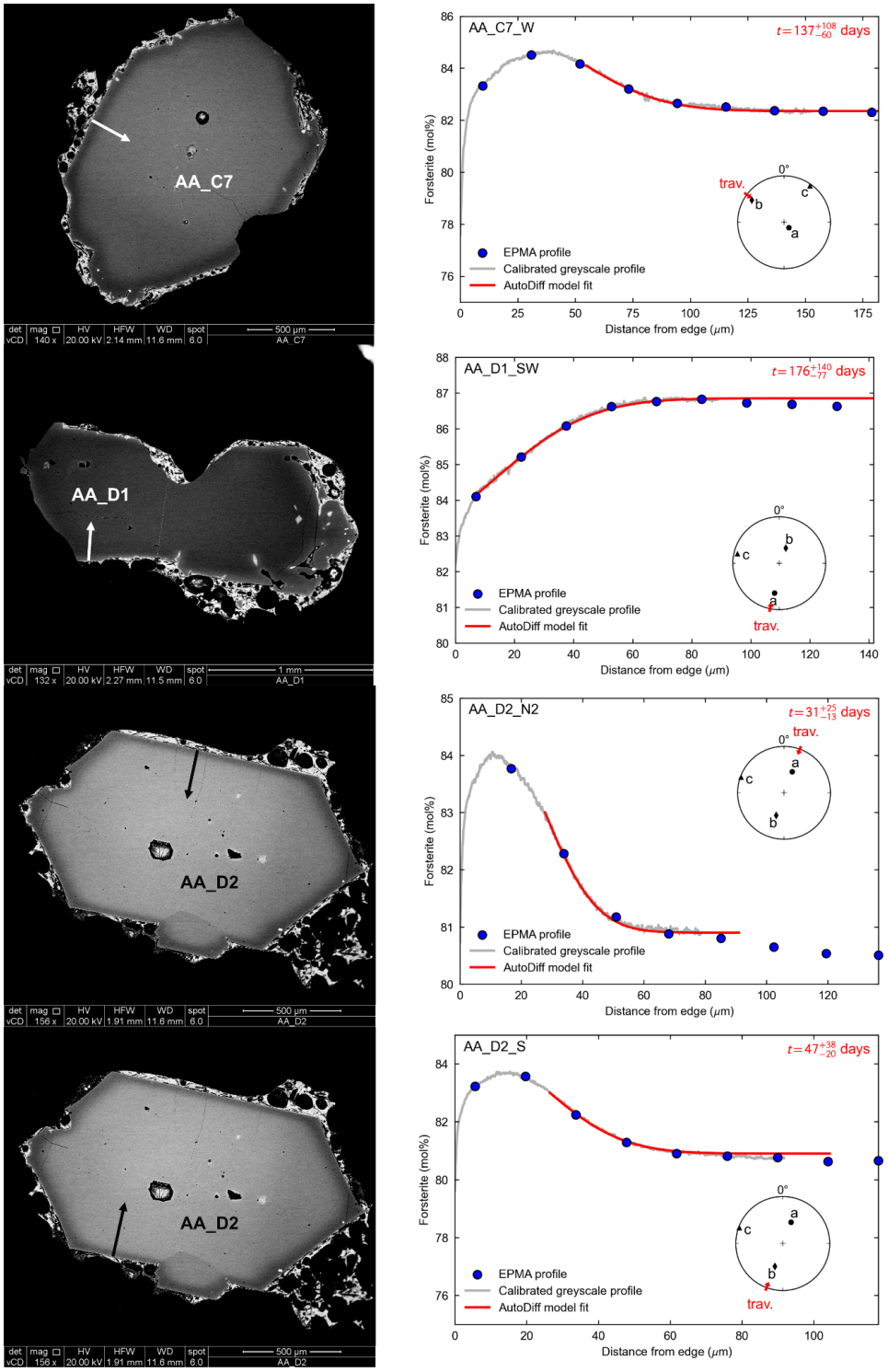
AA_C7
AA_D1
AA_D2
AA_D2
AA_C7_W
$t = 137^{+108}_{-60}$ days
AA_D1_SW
$t = 176^{+140}_{-77}$ days
AA_D2_N2
$t = 31^{+25}_{-13}$ days
AA_D2_S
$t = 47^{+38}_{-20}$ days
Forsterite (mol%)
Distance from edge (μm)
EPMA profile
Calibrated greyscale profile
AutoDiff model fit
trav.

Figure S9.

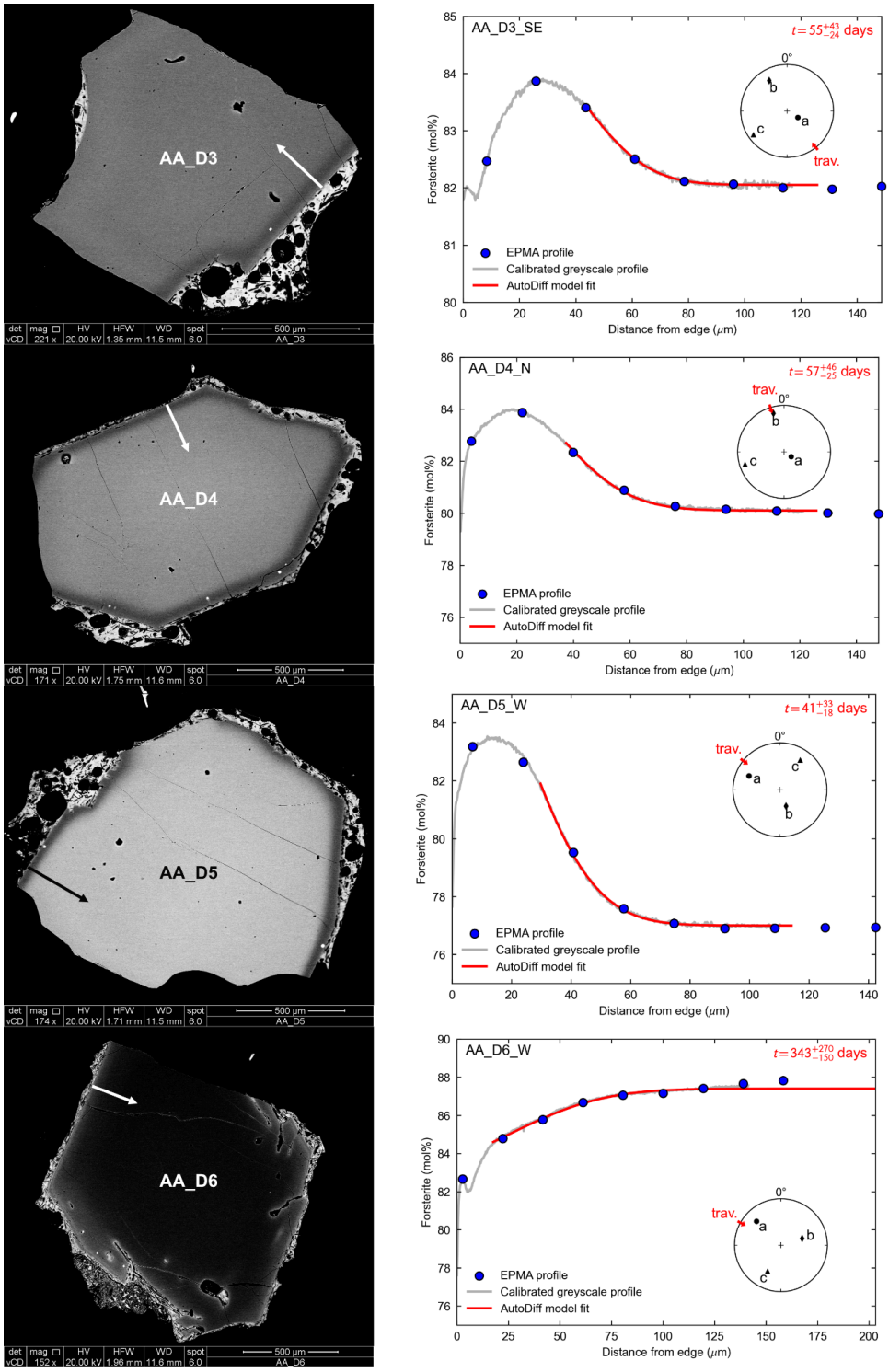
AA_D3
AA_D4
AA_D5
AA_D6
AA_D3_SE
$t = 55^{+43}_{-24}$ days
AA_D4_N
$t = 57^{+46}_{-25}$ days
AA_D5_W
$t = 41^{+33}_{-18}$ days
AA_D6_W
$t = 343^{+270}_{-150}$ days
Forsterite (mol%)
Distance from edge (μm)
EPMA profile
Calibrated greyscale profile
AutoDiff model fit
trav.
0°
a
b
c

Figure S10.

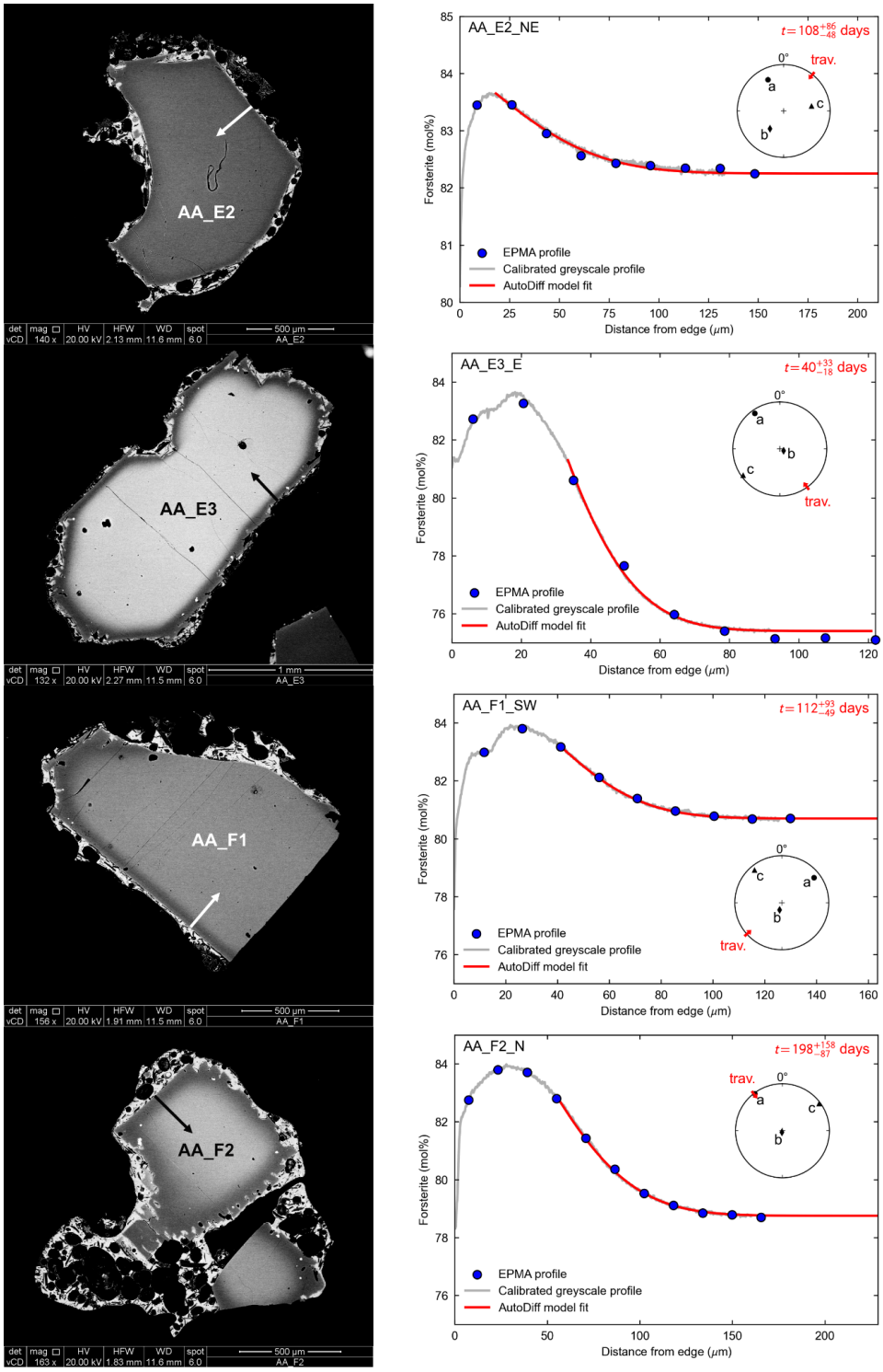
AA_E2
AA_E3
AA_F1
AA_F2
AA_E2_NE
$t = 108^{+86}_{-48}$ days
AA_E3_E
$t = 40^{+33}_{-18}$ days
AA_F1_SW
$t = 112^{+93}_{-49}$ days
AA_F2_N
$t = 198^{+158}_{-87}$ days
Forsterite (mol%)
Distance from edge (μm)
EPMA profile
Calibrated greyscale profile
AutoDiff model fit
trav.
0°
a
b
c

Figure S11.

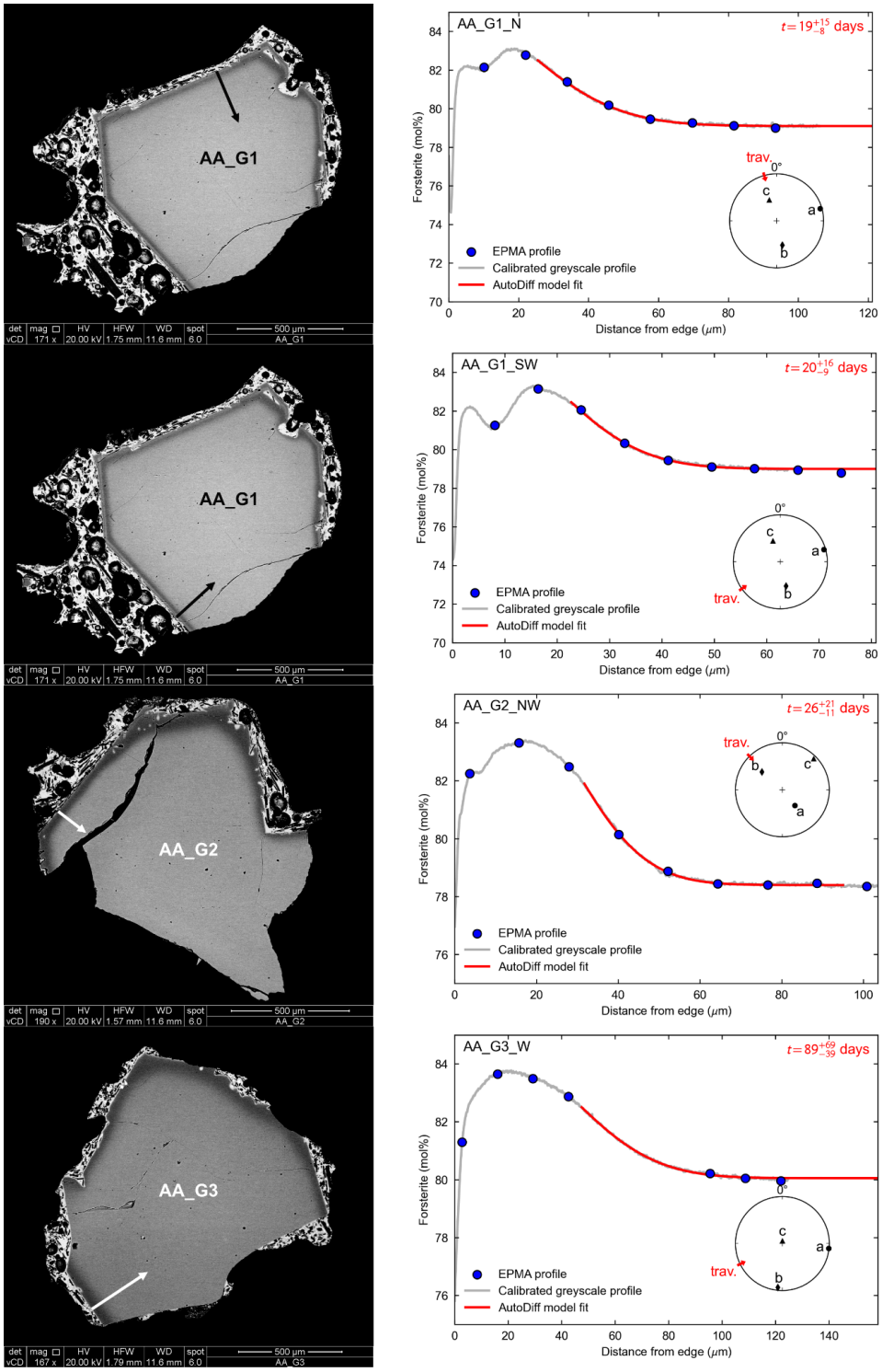
AA_G1
AA_G1
AA_G2
AA_G3
AA_G1_N
$t = 19^{+15}_{-8}$ days
AA_G1_SW
$t = 20^{+16}_{-9}$ days
AA_G2_NW
$t = 26^{+21}_{-11}$ days
AA_G3_W
$t = 89^{+69}_{-39}$ days
Forsterite (mol%)
Distance from edge (μm)
EPMA profile
Calibrated greyscale profile
AutoDiff model fit
trav.
0°
a
b
c

Figure S12.

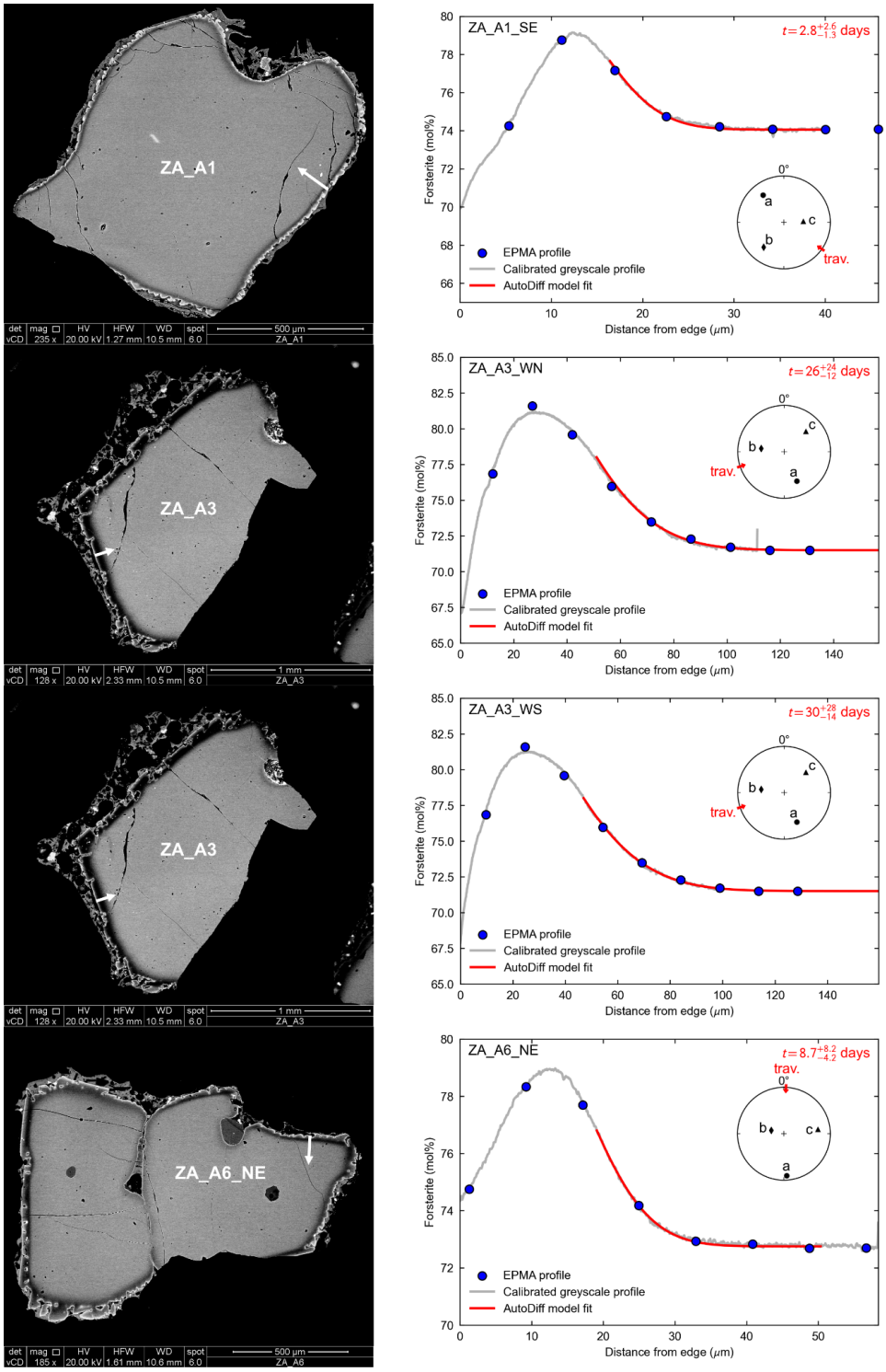
ZA_A1
ZA_A3
ZA_A3
ZA_A6_NE
ZA_A1_SE
$t = 2.8^{+2.6}_{-1.3}$ days
ZA_A3_WN
$t = 26^{+24}_{-12}$ days
ZA_A3_WS
$t = 30^{+28}_{-14}$ days
ZA_A6_NE
$t = 8.7^{+8.2}_{-4.2}$ days
trav.
Forsterite (mol%)
Distance from edge (μm)
EPMA profile
Calibrated greyscale profile
AutoDiff model fit

Figure S13.

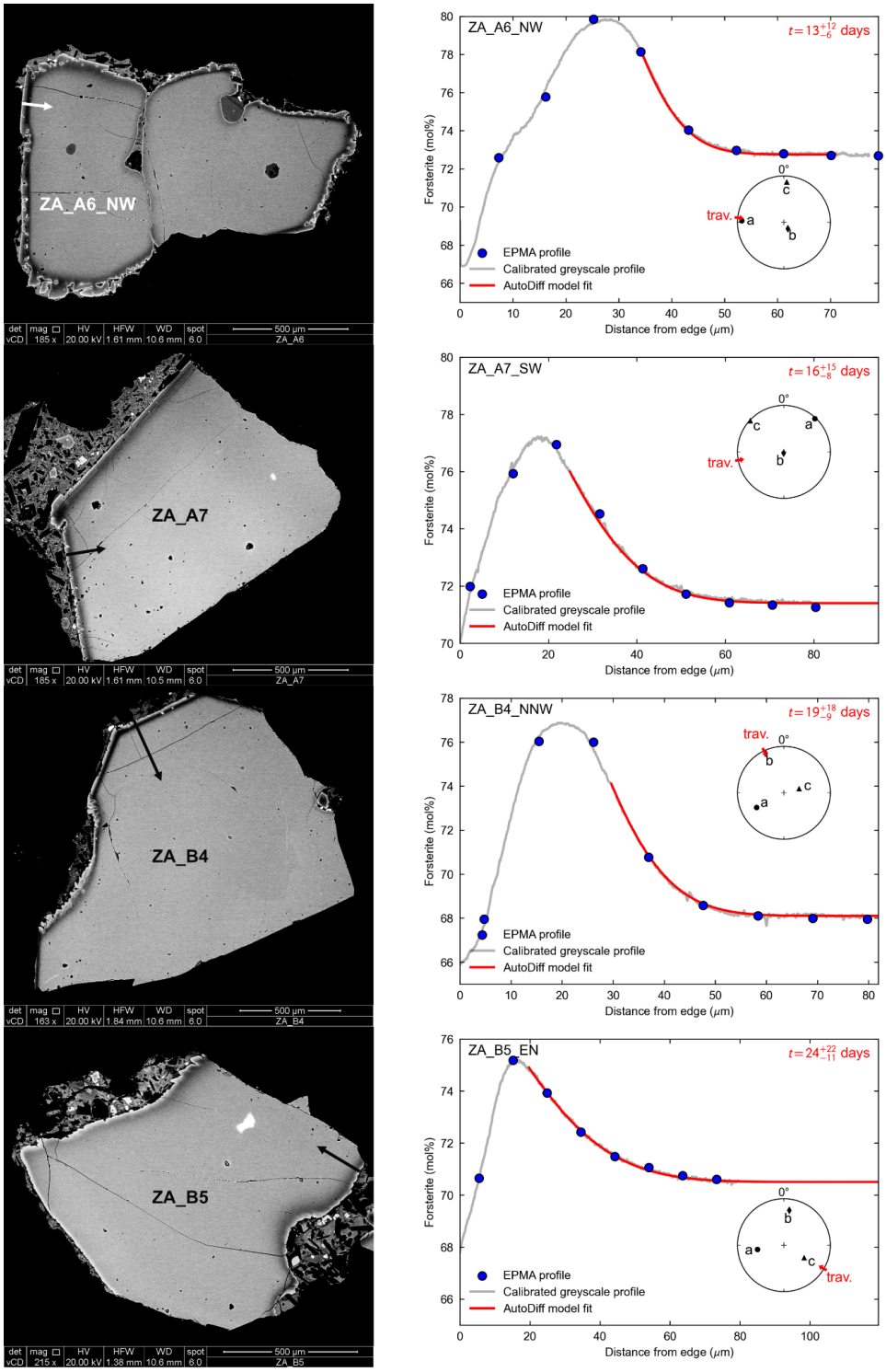
ZA_A6_NW
ZA_A7
ZA_B4
ZA_B5
det mag HV HFW WD spot
vCD 185 x 20.00 kV 1.61 mm 10.6 mm 6.0
500 µm
ZA_A6
vCD 185 x 20.00 kV 1.61 mm 10.5 mm 6.0
ZA_A7
vCD 163 x 20.00 kV 1.84 mm 10.6 mm 6.0
ZA_B4
vCD 215 x 20.00 kV 1.38 mm 10.6 mm 6.0
ZA_B5
ZA_A6_NW
$t = 13^{+12}_{-6}$ days
ZA_A7_SW
$t = 16^{+15}_{-8}$ days
ZA_B4_NNW
$t = 19^{+18}_{-9}$ days
ZA_B5_EN
$t = 24^{+22}_{-11}$ days
Forsterite (mol%)
Distance from edge (µm)
EPMA profile
Calibrated greyscale profile
AutoDiff model fit
trav.
0°
a
b
c

Figure S14.

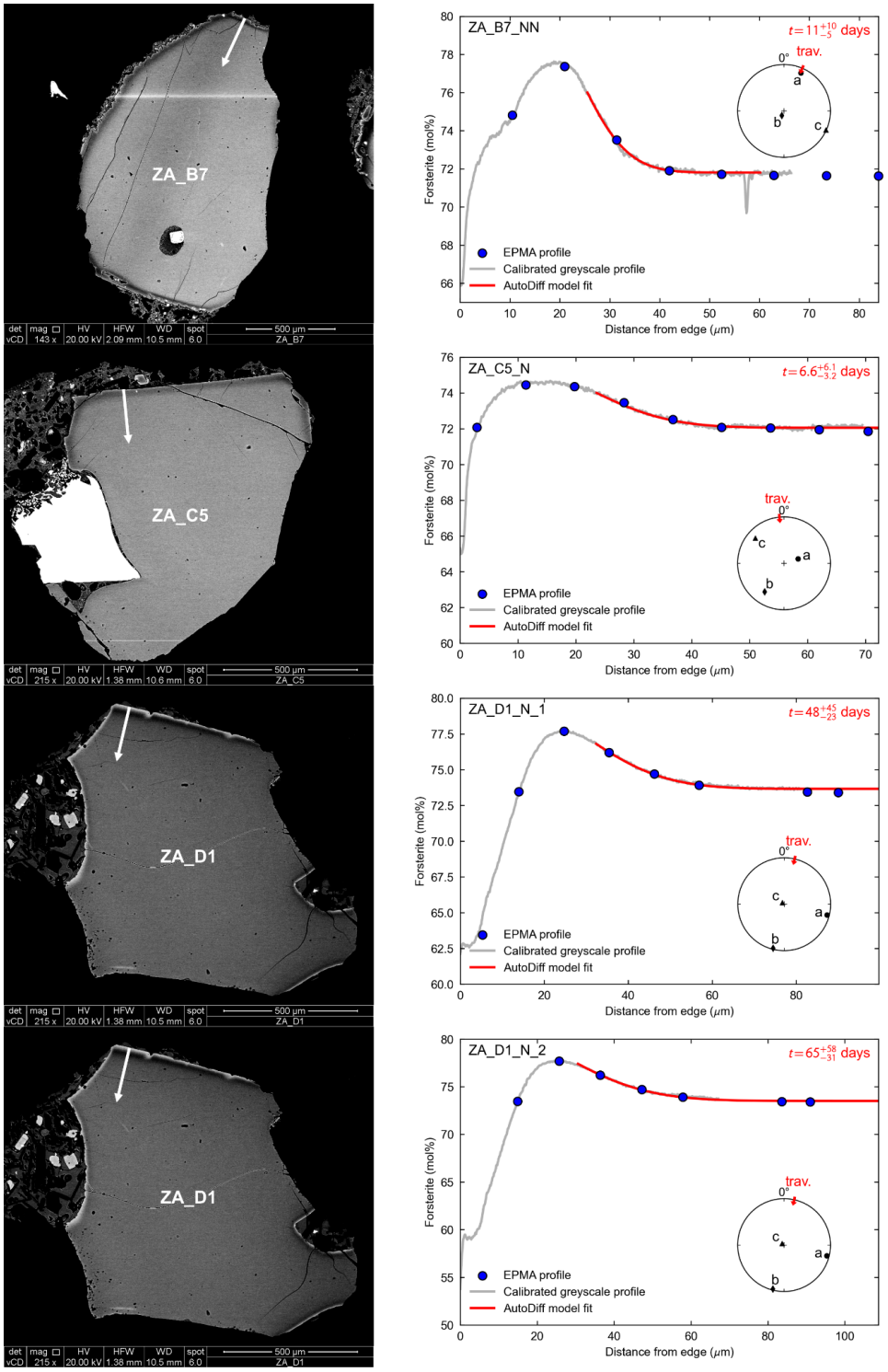
ZA_B7
ZA_C5
ZA_D1
ZA_D1
ZA_B7_NN
$t=11^{+10}_{-5}$ days
ZA_C5_N
$t=6.6^{+6.1}_{-3.2}$ days
ZA_D1_N_1
$t=48^{+45}_{-23}$ days
ZA_D1_N_2
$t=65^{+58}_{-31}$ days
trav.
Forsterite (mol%)
Distance from edge (μm)
EPMA profile
Calibrated greyscale profile
AutoDiff model fit

Figure S15.

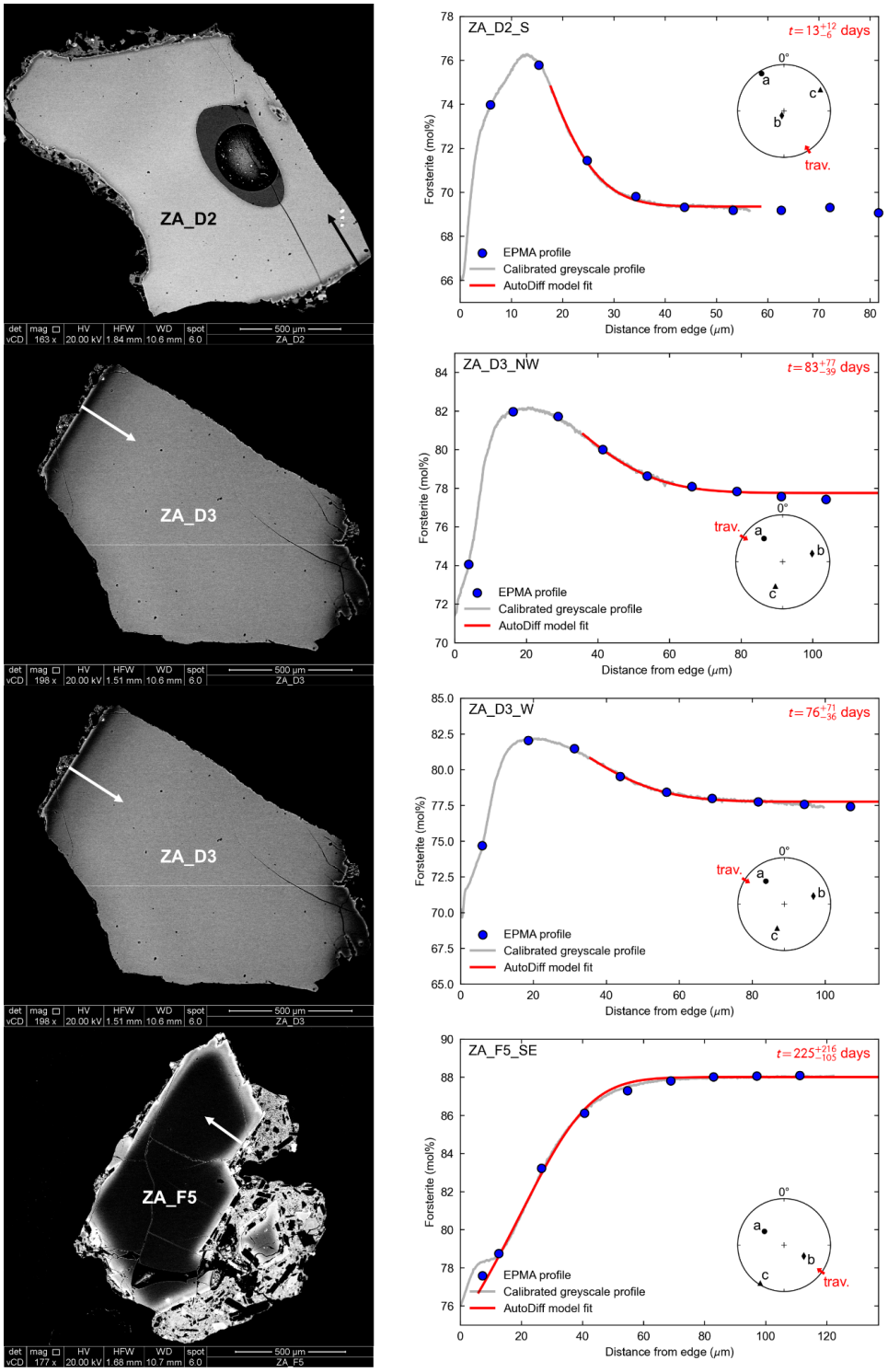
ZA_D2
ZA_D3
ZA_D3
ZA_F5
ZA_D2_S
$t = 13^{+12}_{-6}$ days
ZA_D3_NW
$t = 83^{+77}_{-39}$ days
ZA_D3_W
$t = 76^{+71}_{-36}$ days
ZA_F5_SE
$t = 225^{+216}_{-105}$ days
Forsterite (mol%)
Distance from edge (μm)
EPMA profile
Calibrated greyscale profile
AutoDiff model fit
trav.
0°
a
b
c

Figure S16.

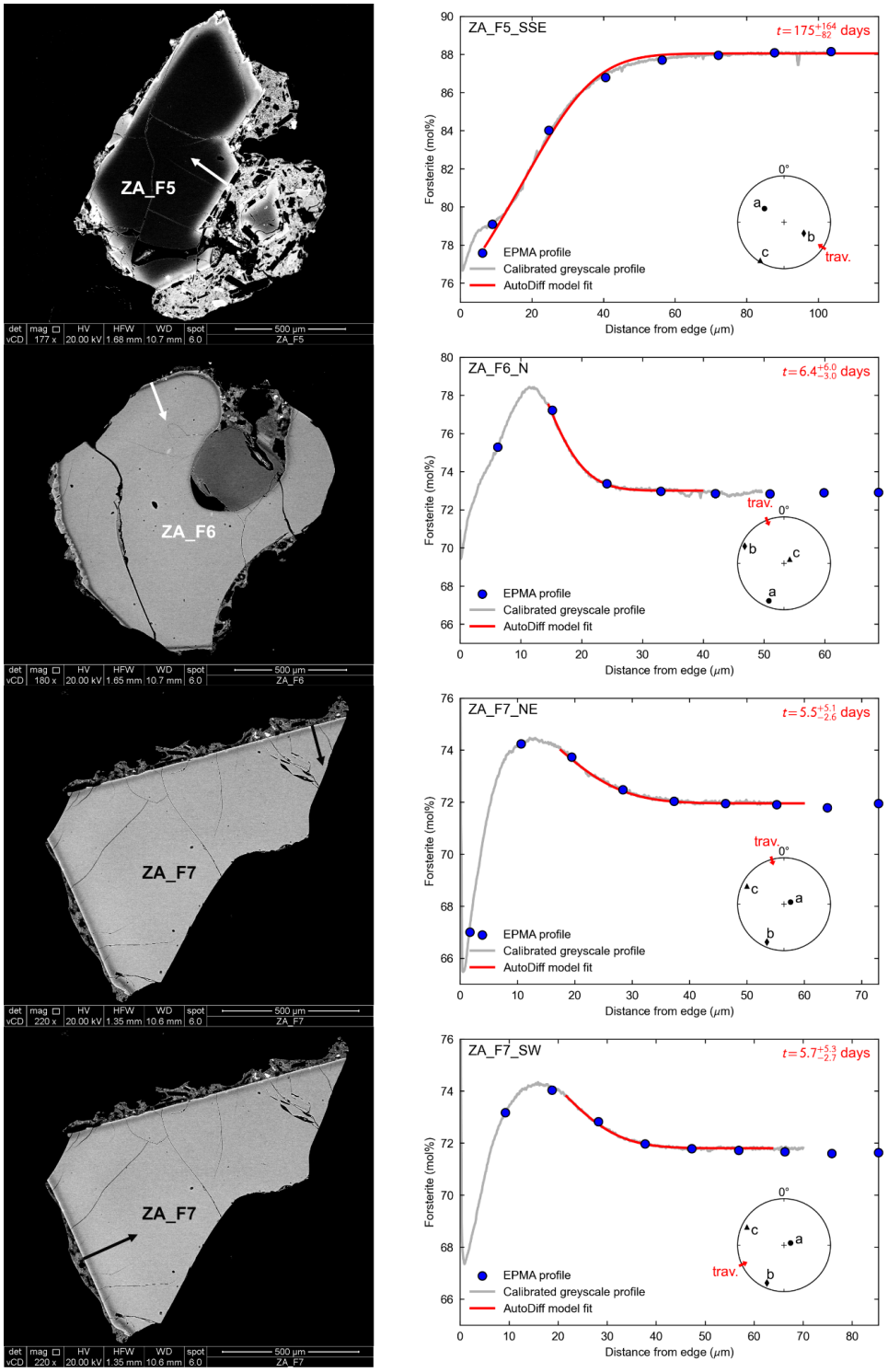
ZA_F5
ZA_F6
ZA_F7
ZA_F7
det mag HV HFW WD spot 500 µm
vCD 177 x 20.00 kV 1.68 mm 10.7 mm 6.0 ZA_F5
vCD 180 x 20.00 kV 1.65 mm 10.7 mm 6.0 ZA_F6
vCD 220 x 20.00 kV 1.35 mm 10.6 mm 6.0 ZA_F7
vCD 220 x 20.00 kV 1.35 mm 10.6 mm 6.0 ZA_F7
ZA_F5_SSE
$t = 175^{+164}_{-82}$ days
ZA_F6_N
$t = 6.4^{+6.0}_{-3.0}$ days
ZA_F7_NE
$t = 5.5^{+5.1}_{-2.6}$ days
ZA_F7_SW
$t = 5.7^{+5.3}_{-2.7}$ days
Forsterite (mol%)
Distance from edge (µm)
EPMA profile
Calibrated greyscale profile
AutoDiff model fit
trav.
0°
a
b
c

Figure S17.

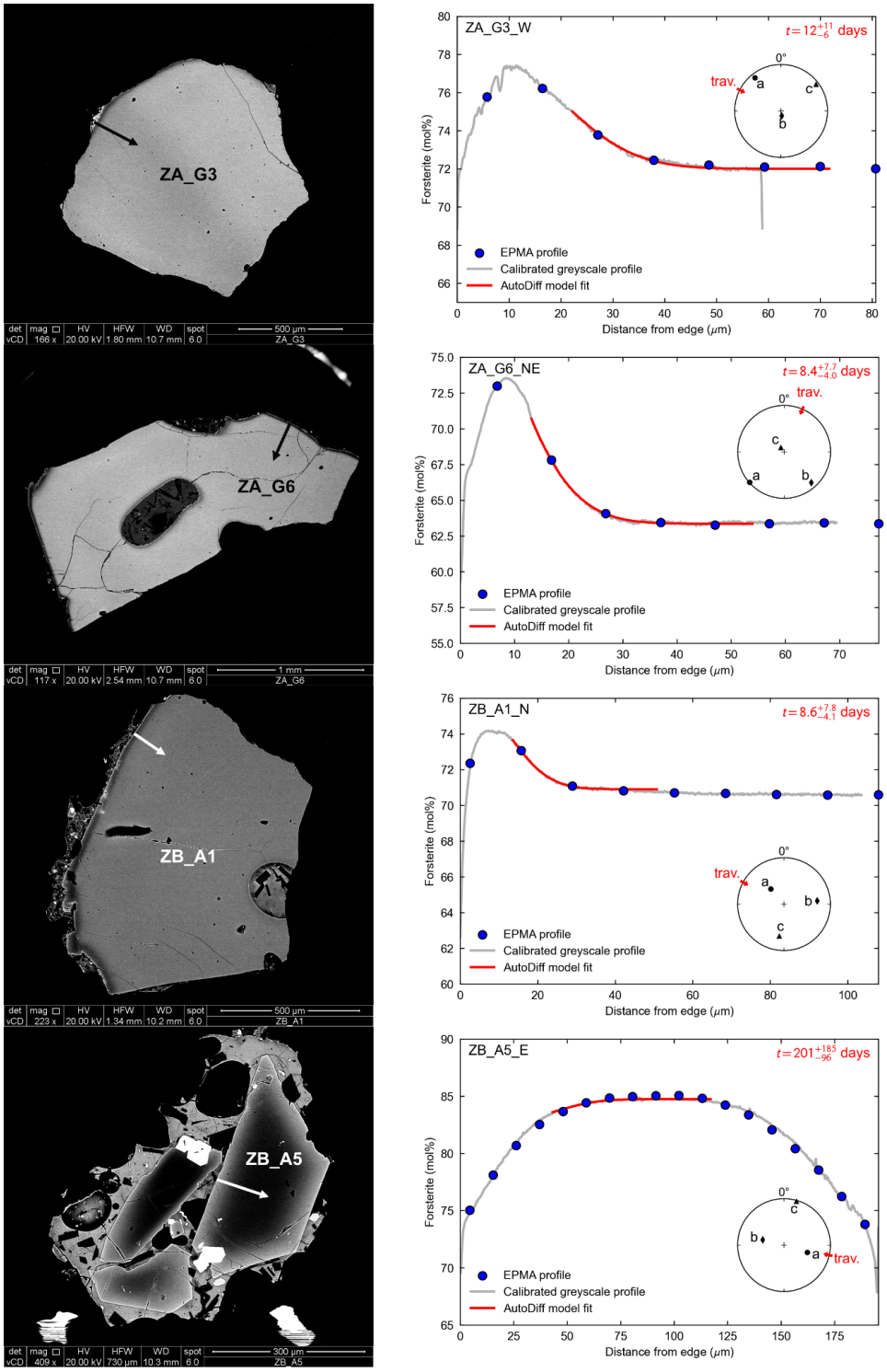
ZA_G3
ZA_G6
ZB_A1
ZB_A5
ZA_G3_W
$t = 12^{+11}_{-6}$ days
ZA_G6_NE
$t = 8.4^{+7.7}_{-4.0}$ days
ZB_A1_N
$t = 8.6^{+7.8}_{-4.1}$ days
ZB_A5_E
$t = 201^{+185}_{-96}$ days
trav.
EPMA profile
Calibrated greyscale profile
AutoDiff model fit
Forsterite (mol%)
Distance from edge (μm)

Figure S18.

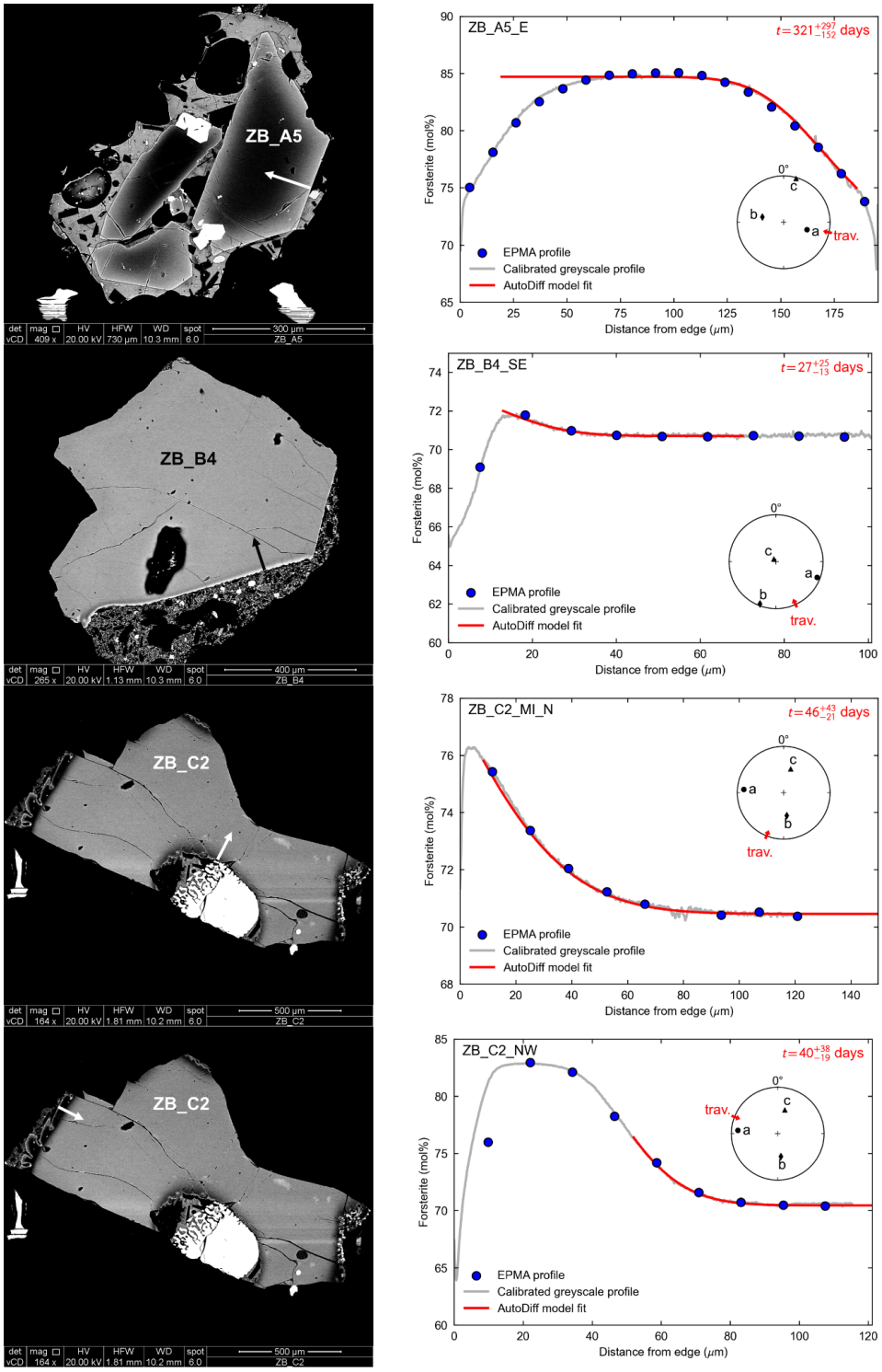
ZB_A5
ZB_B4
ZB_C2
ZB_C2
ZB_A5_E
$t = 321^{+297}_{-152}$ days
ZB_B4_SE
$t = 27^{+25}_{-13}$ days
ZB_C2_MI_N
$t = 46^{+43}_{-21}$ days
ZB_C2_NW
$t = 40^{+38}_{-19}$ days
Forsterite (mol%)
Distance from edge (μm)
EPMA profile
Calibrated greyscale profile
AutoDiff model fit
trav.
0°
a
b
c

Figure S19.

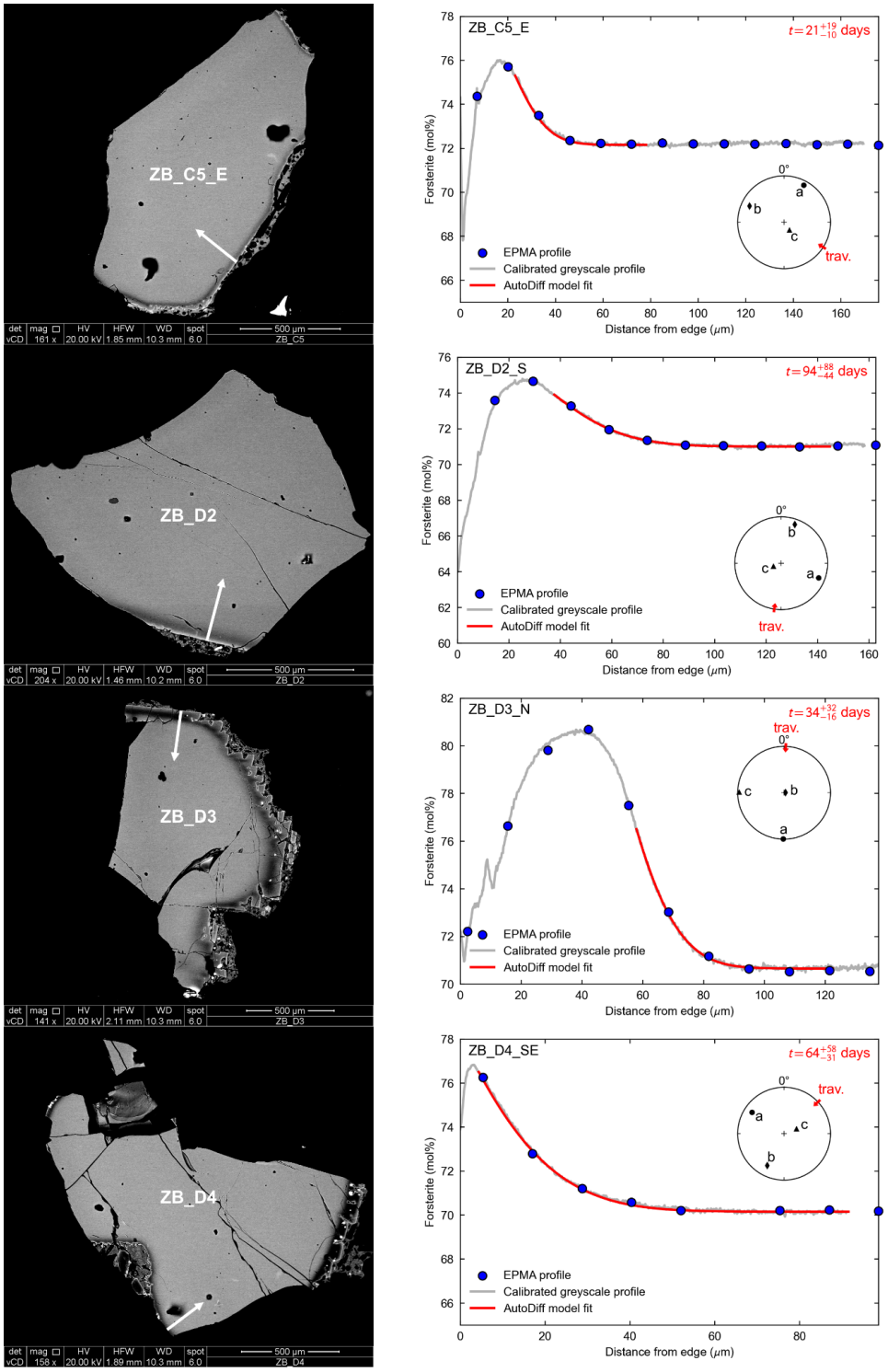
ZB_C5_E
ZB_D2
ZB_D3
ZB_D4
ZB_C5_E
$t = 21^{+19}_{-10}$ days
ZB_D2_S
$t = 94^{+88}_{-44}$ days
ZB_D3_N
$t = 34^{+32}_{-16}$ days
ZB_D4_SE
$t = 64^{+58}_{-31}$ days
Forsterite (mol%)
Distance from edge (μm)
EPMA profile
Calibrated greyscale profile
AutoDiff model fit
trav.

Figure S20.

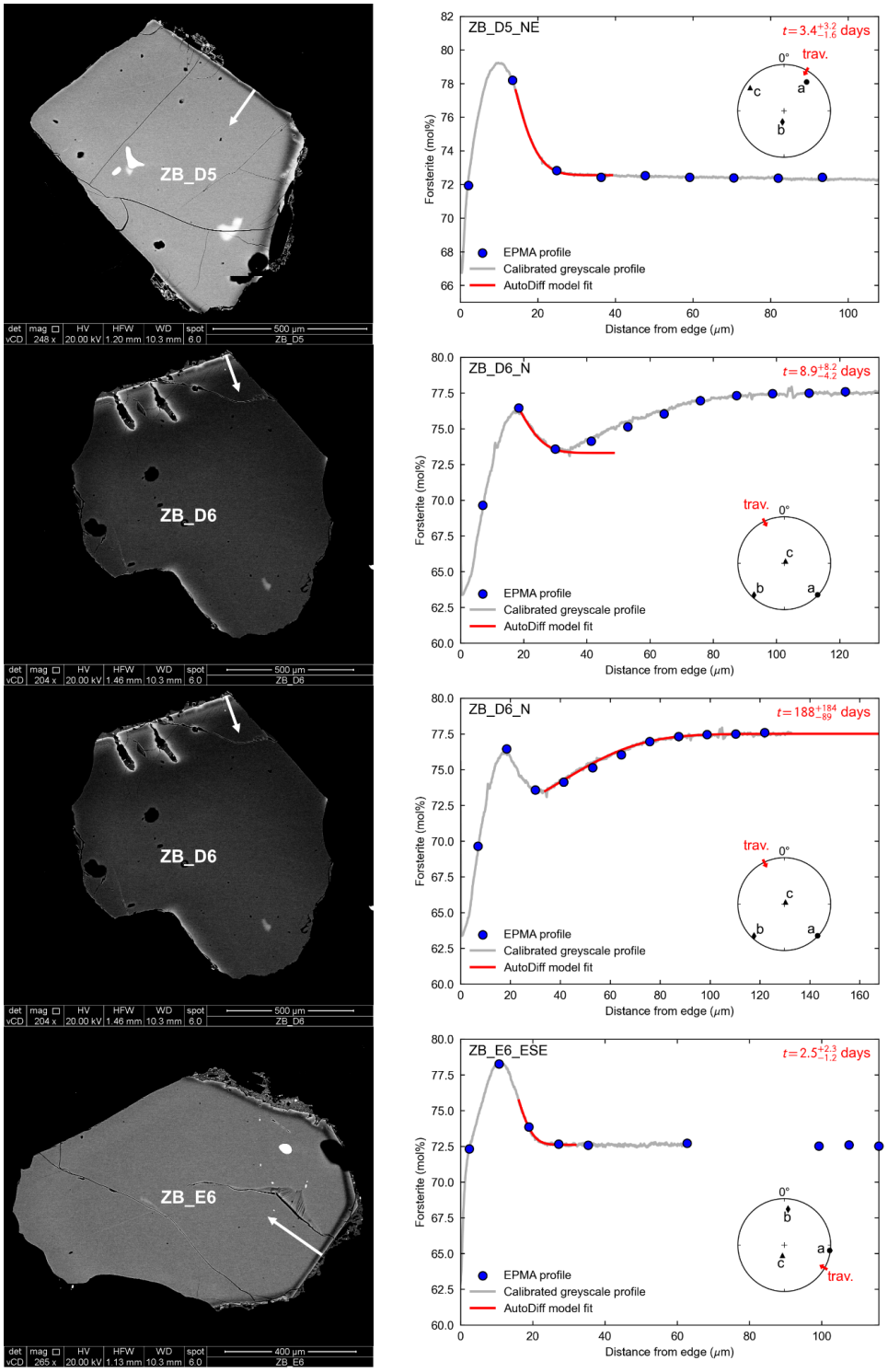
ZB_D5
ZB_D6
ZB_D6
ZB_E6
ZB_D5_NE
$t = 3.4^{+3.2}_{-1.6}$ days
trav.
ZB_D6_N
$t = 8.9^{+8.2}_{-4.2}$ days
ZB_D6_N
$t = 188^{+184}_{-89}$ days
ZB_E6_ESE
$t = 2.5^{+2.3}_{-1.2}$ days
Forsterite (mol%)
Distance from edge (μm)
EPMA profile
Calibrated greyscale profile
AutoDiff model fit

Figure S21.

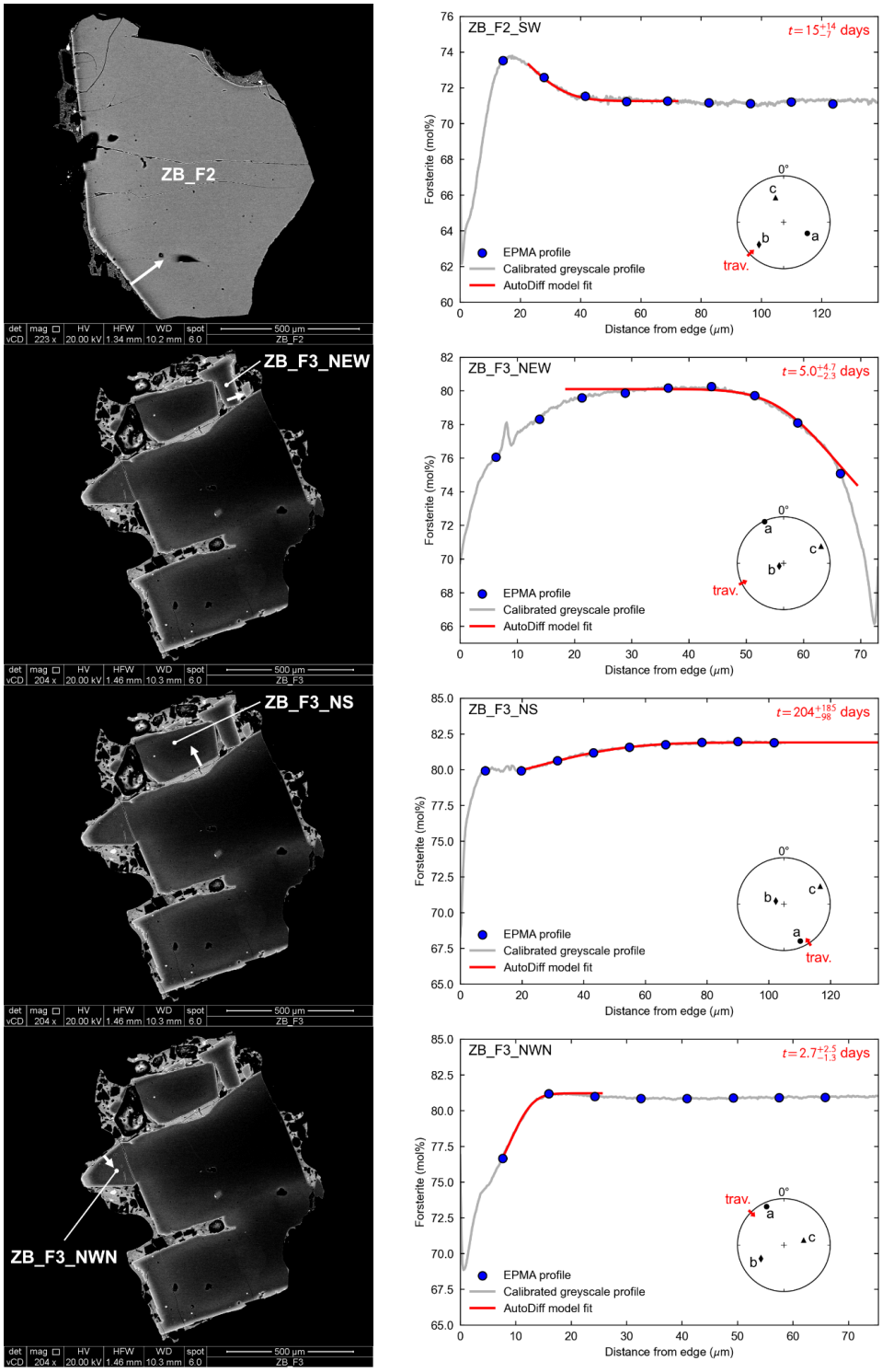
ZB_F2
ZB_F3_NEW
ZB_F3_NS
ZB_F3_NWN
ZB_F2_SW
$t = 15^{+14}_{-7}$ days
ZB_F3_NEW
$t = 5.0^{+4.7}_{-2.3}$ days
ZB_F3_NS
$t = 204^{+185}_{-98}$ days
ZB_F3_NWN
$t = 2.7^{+2.5}_{-1.3}$ days
Forsterite (mol%)
Distance from edge (μm)
EPMA profile
Calibrated greyscale profile
AutoDiff model fit
trav.

Figure S22.

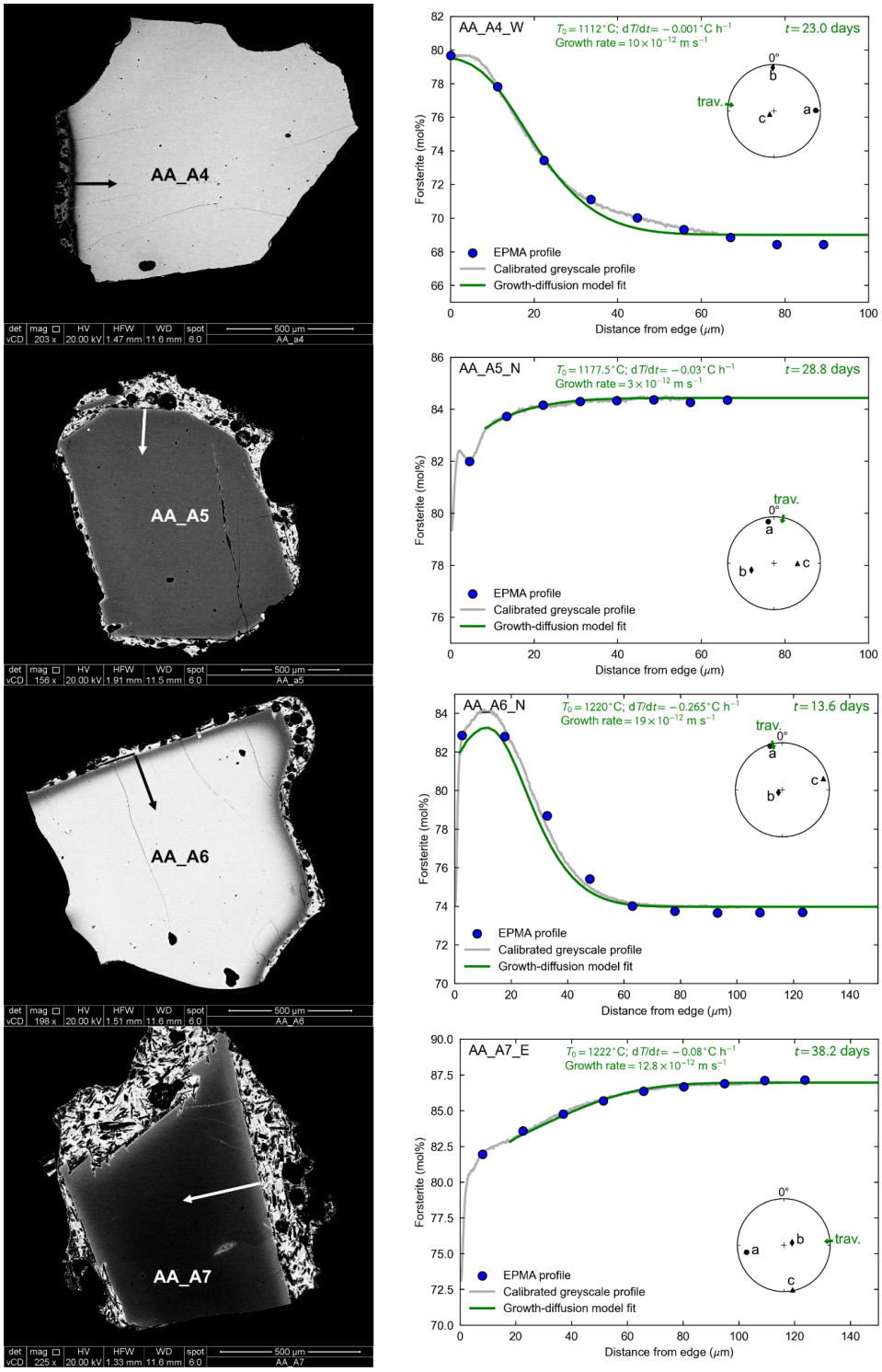

Figures S23–S30: Backscatter electron images showing profile traverses across Main Ethiopian Rift olivines, and plots showing Fo change with traverse distance across profiles. Growth-diffusion model fits are shown as the green line, and variables are shown as the green text. Pole figures showing crystallographic orientation are shown as inset figures.

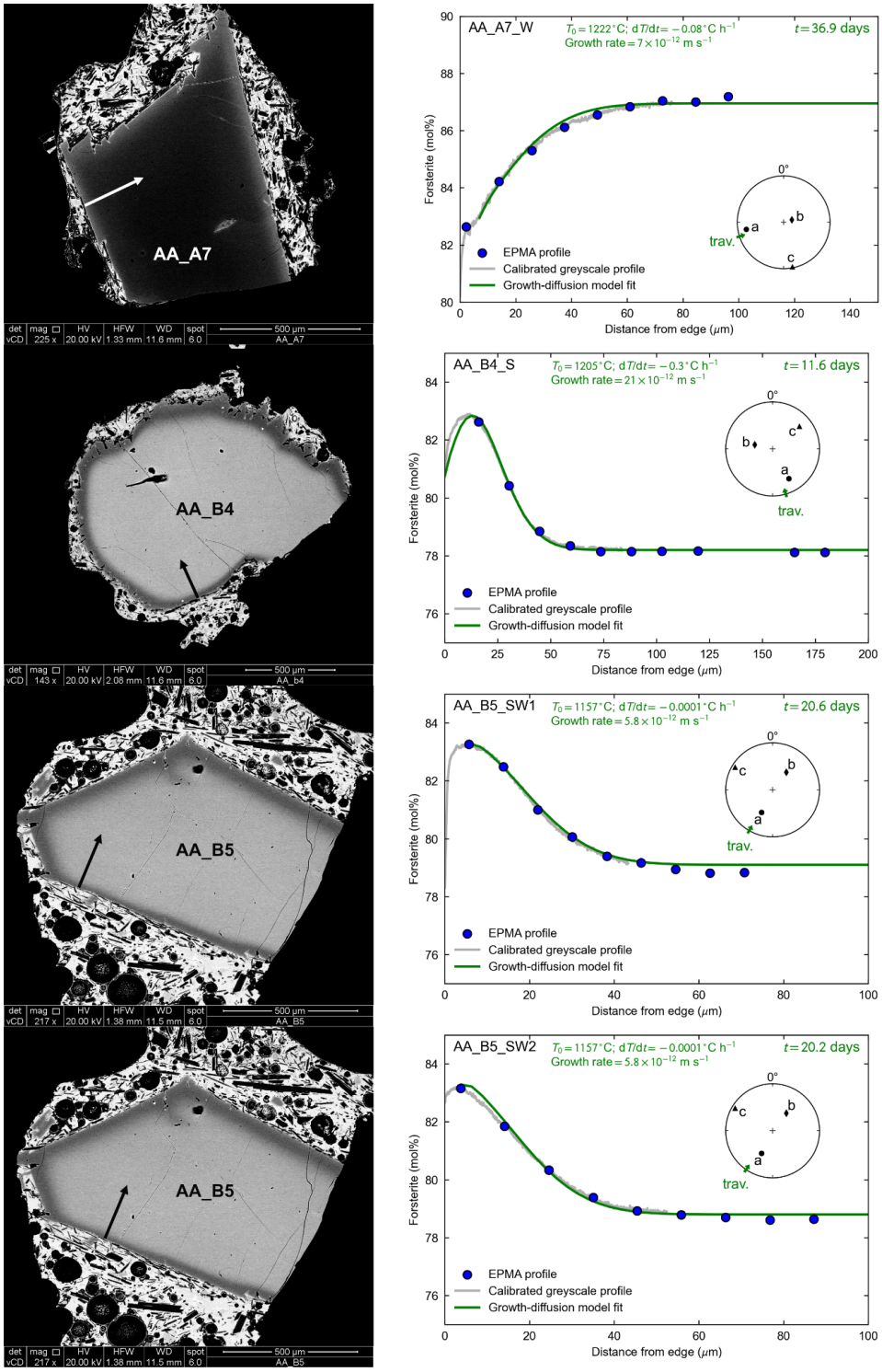
AA_A7
AA_B4
AA_B5
AA_B5
AA_A7_W
$T_0 = 1222$ °C; dT/dt = −0.08 °C h^{-1}
Growth rate = 7 × 10^{-12} m s^{-1}
t = 36.9 days
AA_B4_S
$T_0 = 1205$ °C; dT/dt = −0.3 °C h^{-1}
Growth rate = 21 × 10^{-12} m s^{-1}
t = 11.6 days
AA_B5_SW1
$T_0 = 1157$ °C; dT/dt = −0.0001 °C h^{-1}
Growth rate = 5.8 × 10^{-12} m s^{-1}
t = 20.6 days
AA_B5_SW2
$T_0 = 1157$ °C; dT/dt = −0.0001 °C h^{-1}
Growth rate = 5.8 × 10^{-12} m s^{-1}
t = 20.2 days
Forsterite (mol%)
Distance from edge (μm)
EPMA profile
Calibrated greyscale profile
Growth-diffusion model fit
trav.

Figure S24.

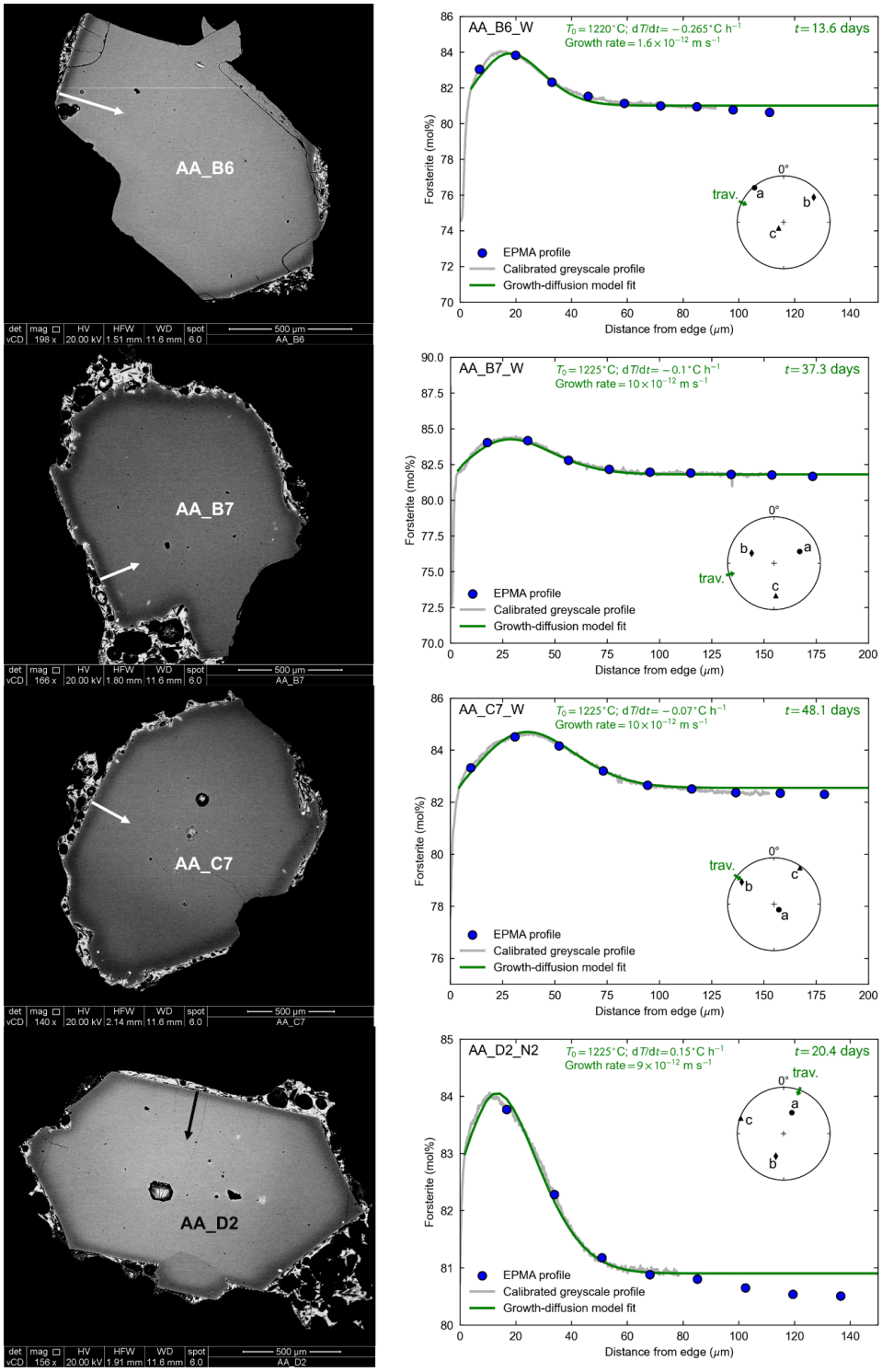
AA_B6
AA_B7
AA_C7
AA_D2
AA_B6_W
$T_0 = 1220$°C; dT/dt = −0.265°C h^{-1}
Growth rate = 1.6 × 10^{-12} m s^{-1}
t = 13.6 days
AA_B7_W
$T_0 = 1225$°C; dT/dt = −0.1°C h^{-1}
Growth rate = 10 × 10^{-12} m s^{-1}
t = 37.3 days
AA_C7_W
$T_0 = 1225$°C; dT/dt = −0.07°C h^{-1}
Growth rate = 10 × 10^{-12} m s^{-1}
t = 48.1 days
AA_D2_N2
$T_0 = 1225$°C; dT/dt = 0.15°C h^{-1}
Growth rate = 9 × 10^{-12} m s^{-1}
t = 20.4 days
Forsterite (mol%)
Distance from edge (μm)
EPMA profile
Calibrated greyscale profile
Growth-diffusion model fit
trav.
0°
a
b
c

Figure S25.

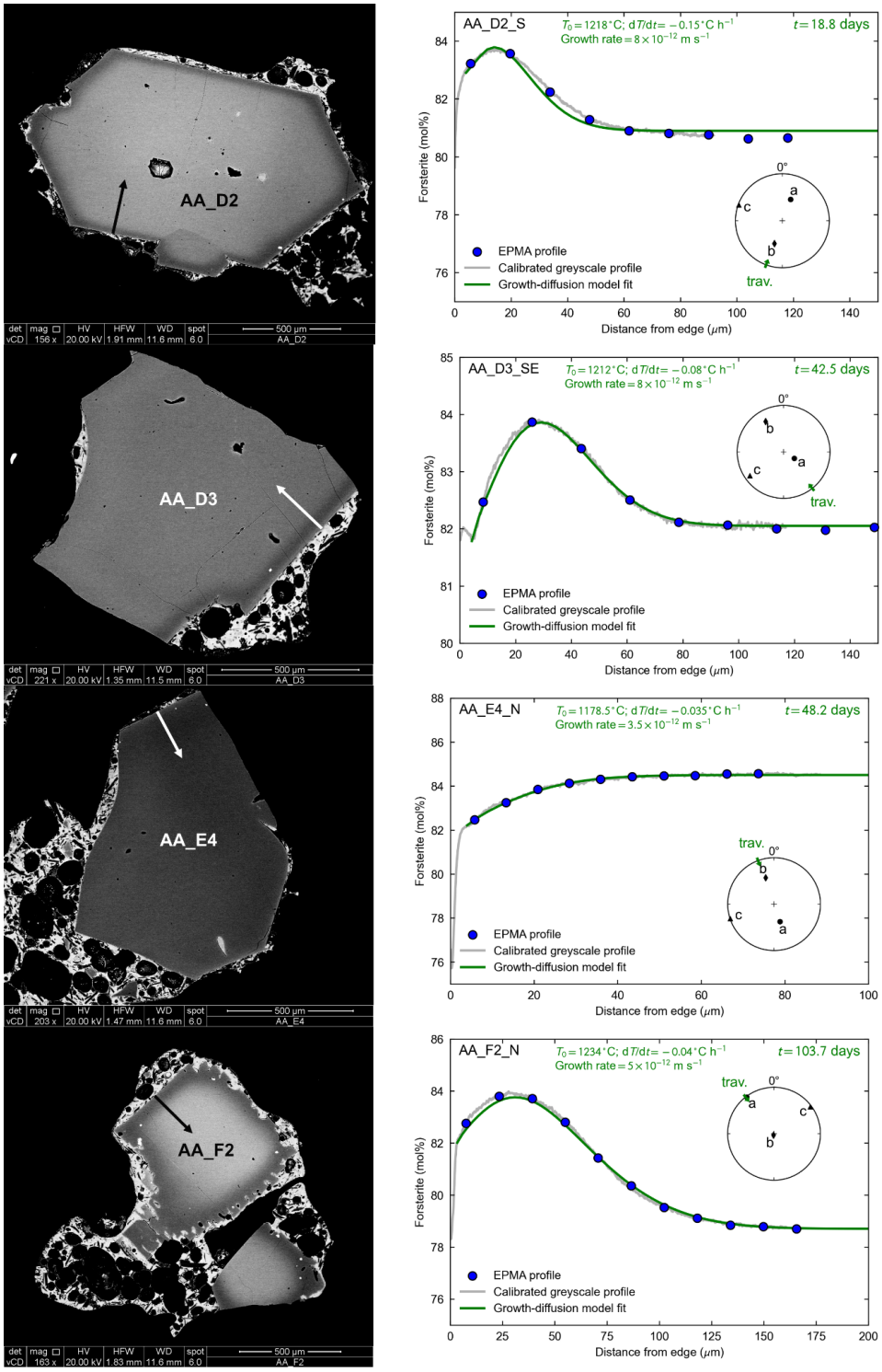
AA_D2
det mag HV HFW WD spot 500 µm
vCD 156 x 20.00 kV 1.91 mm 11.6 mm 6.0 AA_D2
AA_D2_S
T_0 = 1218 °C; dT/dt = −0.15 °C h^{-1}
Growth rate = 8 × 10^{-12} m s^{-1}
t = 18.8 days
Forsterite (mol%)
Distance from edge (µm)
EPMA profile
Calibrated greyscale profile
Growth-diffusion model fit
0°
a
b
c
trav.
AA_D3
det mag HV HFW WD spot 500 µm
vCD 221 x 20.00 kV 1.35 mm 11.5 mm 6.0 AA_D3
AA_D3_SE
T_0 = 1212 °C; dT/dt = −0.08 °C h^{-1}
Growth rate = 8 × 10^{-12} m s^{-1}
t = 42.5 days
AA_E4
det mag HV HFW WD spot 500 µm
vCD 203 x 20.00 kV 1.47 mm 11.6 mm 6.0 AA_E4
AA_E4_N
T_0 = 1178.5 °C; dT/dt = −0.035 °C h^{-1}
Growth rate = 3.5 × 10^{-12} m s^{-1}
t = 48.2 days
AA_F2
det mag HV HFW WD spot 500 µm
vCD 163 x 20.00 kV 1.83 mm 11.6 mm 6.0 AA_F2
AA_F2_N
T_0 = 1234 °C; dT/dt = −0.04 °C h^{-1}
Growth rate = 5 × 10^{-12} m s^{-1}
t = 103.7 days

Figure S26.

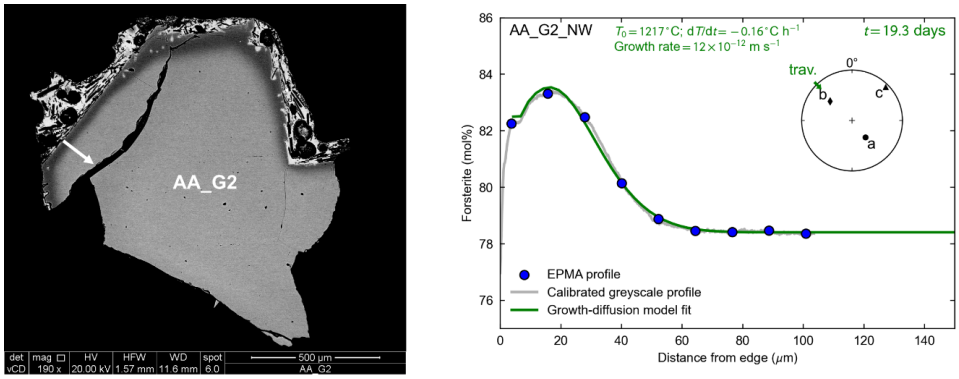
AA_G2
det mag HV HFW WD spot
vCD 190 x 20.00 kV 1.57 mm 11.6 mm 6.0
500 µm
AA_G2
AA_G2_NW
T_0 = 1217 °C; dT/dt = −0.16 °C h^{-1}
Growth rate = 12 × 10^{-12} m s^{-1}
t = 19.3 days
trav.
0°
b
c
a
Forsterite (mol%)
86
84
82
80
78
76
0
20
40
60
80
100
120
140
Distance from edge (µm)
EPMA profile
Calibrated greyscale profile
Growth-diffusion model fit

Figure S27.

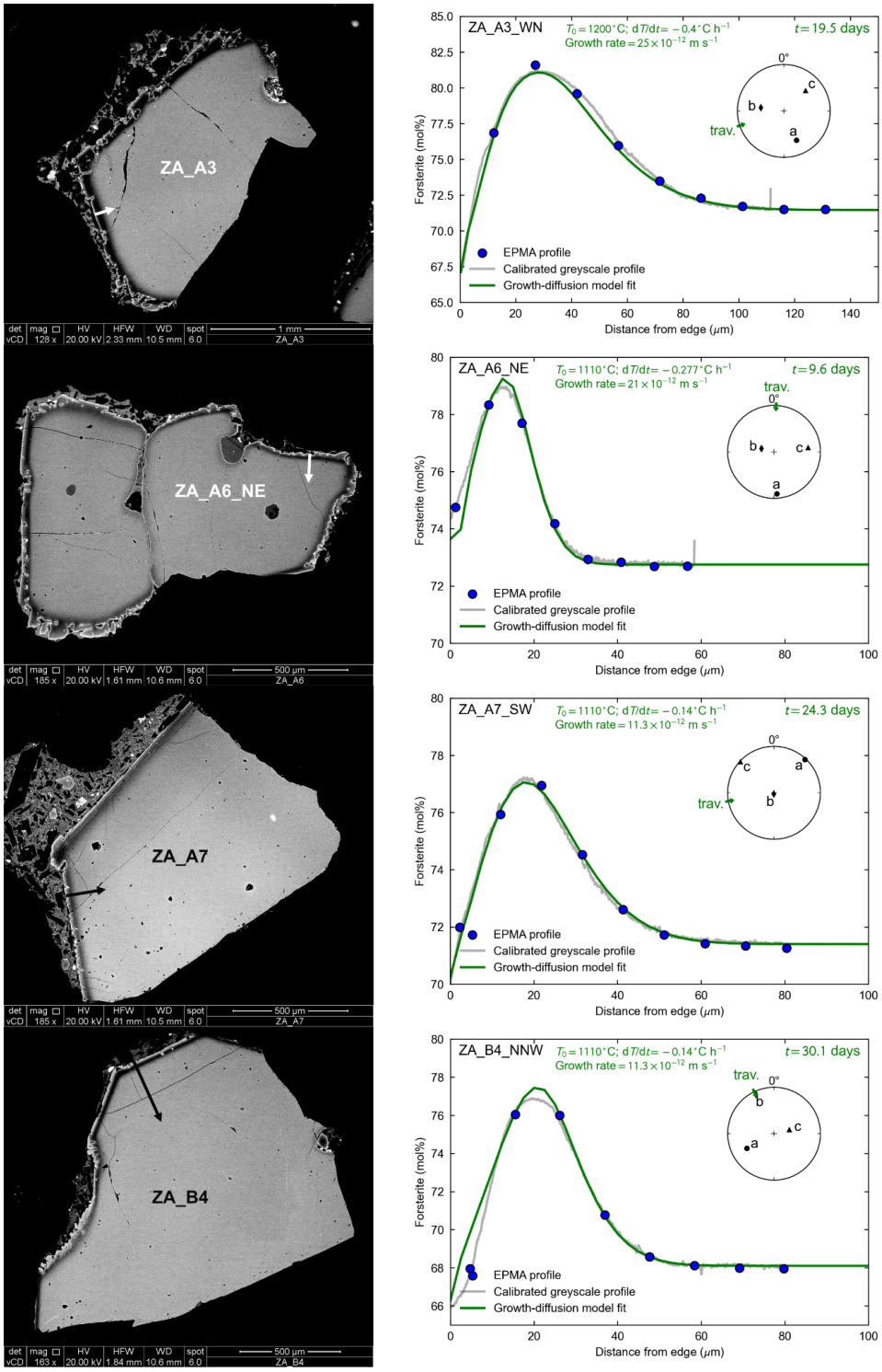
ZA_A3
det mag HV HFW WD spot
vCD 128 x 20.00 kV 2.33 mm 10.5 mm 6.0
1 mm
ZA_A3
ZA_A6_NE
det mag HV HFW WD spot
vCD 185 x 20.00 kV 1.61 mm 10.6 mm 6.0
500 µm
ZA_A6
ZA_A7
det mag HV HFW WD spot
vCD 185 x 20.00 kV 1.61 mm 10.5 mm 6.0
500 µm
ZA_A7
ZA_B4
det mag HV HFW WD spot
vCD 163 x 20.00 kV 1.84 mm 10.6 mm 6.0
500 µm
ZA_B4
ZA_A3_WN
T_0 = 1200°C; dT/dt = −0.4°C h^{-1}
Growth rate = 25 × 10^{-12} m s^{-1}
t = 19.5 days
ZA_A6_NE
T_0 = 1110°C; dT/dt = −0.277°C h^{-1}
Growth rate = 21 × 10^{-12} m s^{-1}
t = 9.6 days
ZA_A7_SW
T_0 = 1110°C; dT/dt = −0.14°C h^{-1}
Growth rate = 11.3 × 10^{-12} m s^{-1}
t = 24.3 days
ZA_B4_NNW
T_0 = 1110°C; dT/dt = −0.14°C h^{-1}
Growth rate = 11.3 × 10^{-12} m s^{-1}
t = 30.1 days
trav.
0°
a
b
c
EPMA profile
Calibrated greyscale profile
Growth-diffusion model fit
Forsterite (mol%)
Distance from edge (µm)

Figure S28.

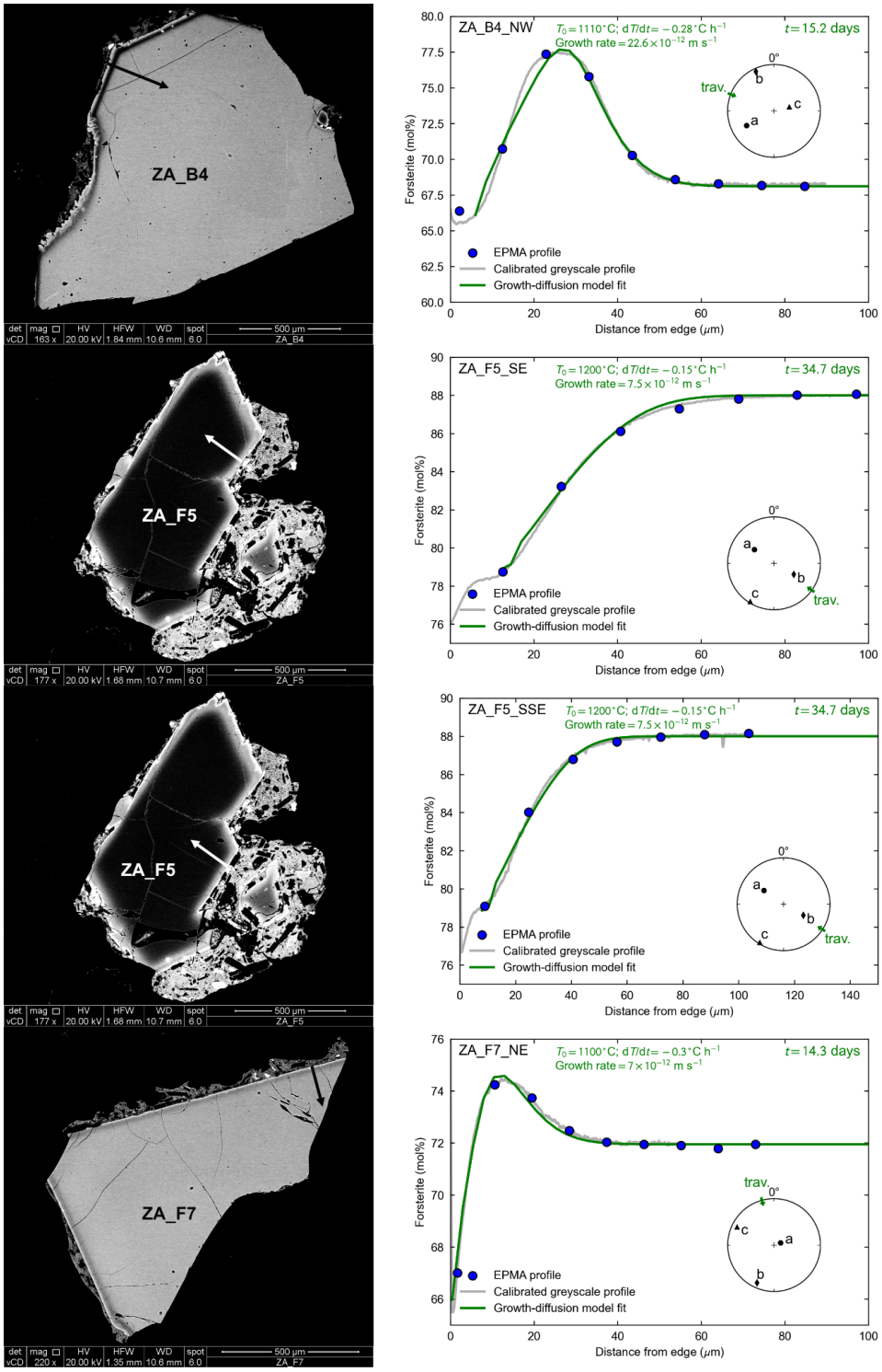
ZA_B4
det mag HV HFW WD spot
vCD 163 x 20.00 kV 1.84 mm 10.6 mm 6.0
500 µm
ZA_B4
ZA_F5
det mag HV HFW WD spot
vCD 177 x 20.00 kV 1.68 mm 10.7 mm 6.0
500 µm
ZA_F5
ZA_F5
det mag HV HFW WD spot
vCD 177 x 20.00 kV 1.68 mm 10.7 mm 6.0
500 µm
ZA_F5
ZA_F7
det mag HV HFW WD spot
vCD 220 x 20.00 kV 1.35 mm 10.6 mm 6.0
500 µm
ZA_F7
ZA_B4_NW
$T_0 = 1110$°C; dT/dt = −0.28°C h^{-1}
Growth rate = 22.6 × 10^{-12} m s^{-1}
t = 15.2 days
trav.
0°
a
b
c
Forsterite (mol%)
Distance from edge (µm)
EPMA profile
Calibrated greyscale profile
Growth-diffusion model fit
ZA_F5_SE
$T_0 = 1200$°C; dT/dt = −0.15°C h^{-1}
Growth rate = 7.5 × 10^{-12} m s^{-1}
t = 34.7 days
ZA_F5_SSE
$T_0 = 1200$°C; dT/dt = −0.15°C h^{-1}
Growth rate = 7.5 × 10^{-12} m s^{-1}
t = 34.7 days
ZA_F7_NE
$T_0 = 1100$°C; dT/dt = −0.3°C h^{-1}
Growth rate = 7 × 10^{-12} m s^{-1}
t = 14.3 days

Figure S29.

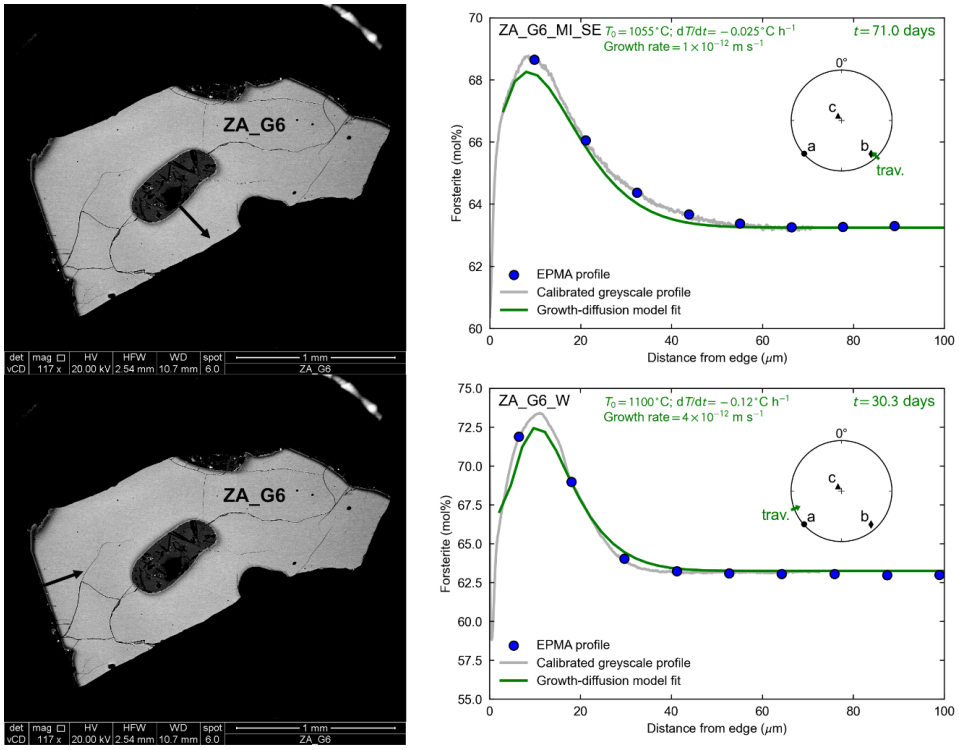
ZA_G6
det mag HV HFW WD spot
vCD 117 x 20.00 kV 2.54 mm 10.7 mm 6.0
1 mm
ZA_G6
ZA_G6_MI_SE $T_0 = 1055$°C; $dT/dt = -0.025$°C h^{-1}
Growth rate = 1×10^{-12} m s^{-1}
$t = 71.0$ days
0°
c
a
b
trav.
Forsterite (mol%)
EPMA profile
Calibrated greyscale profile
Growth-diffusion model fit
Distance from edge (μm)
ZA_G6_W $T_0 = 1100$°C; $dT/dt = -0.12$°C h^{-1}
Growth rate = 4×10^{-12} m s^{-1}
$t = 30.3$ days

Figure S30.

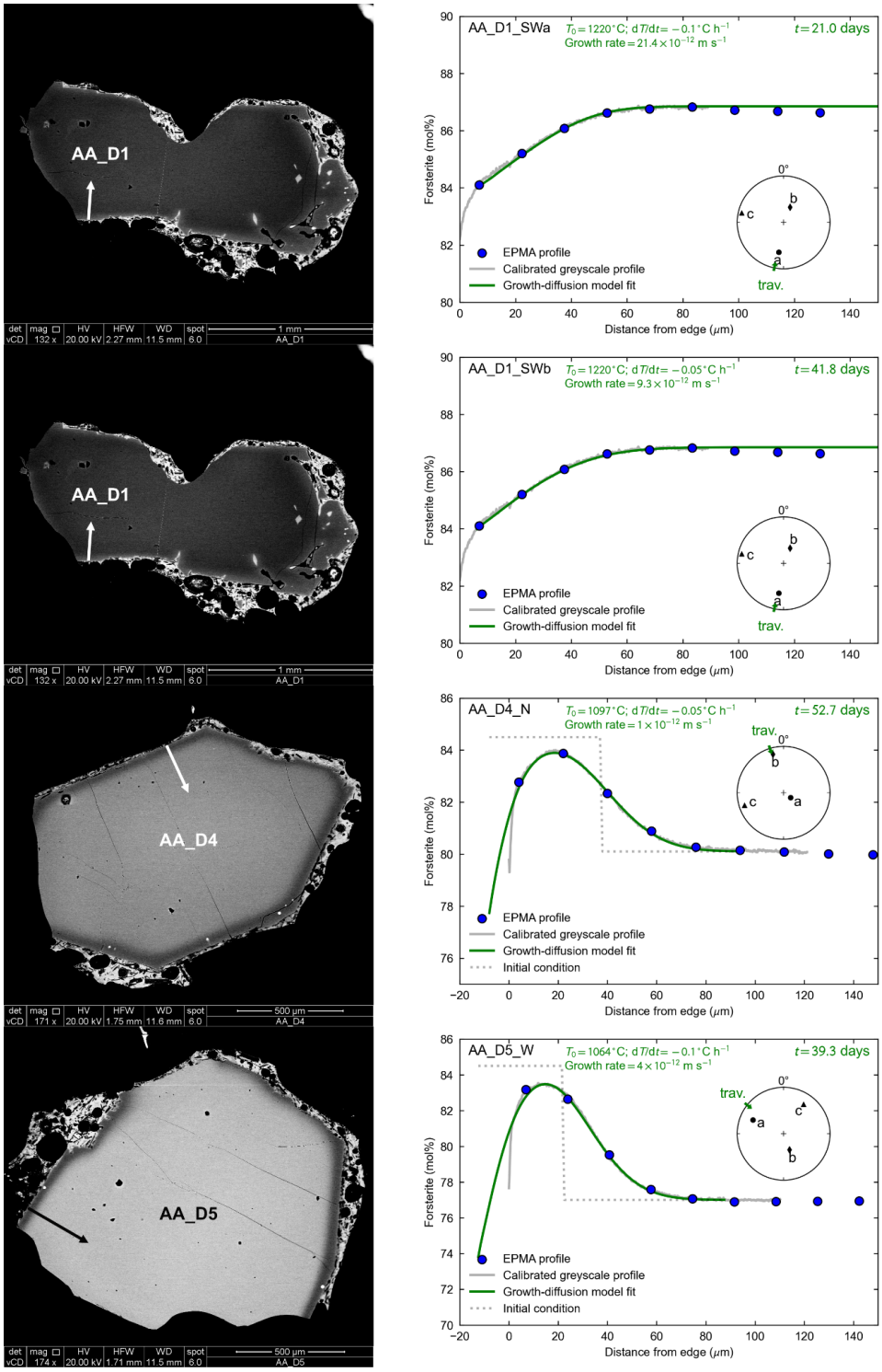

Figure S31: Growth-diffusion models as shown in Figures S23–S30, but for unique cases. The top two figures are two fits to the greyscale profile. However, their input variables are different, resulting in two different timescales. The bottom two figures are cases where a stepped initial profile is assumed, in contrast to the core plateau starting profile in all other cases.

References for figure captions

1. Gualda, G. A. R., Ghiorso, M. S., Lemons, R. V. & Carley, T. L. Rhyolite-MELTS: a Modified Calibration of MELTS Optimized for Silica-rich, Fluid-bearing Magmatic Systems. *J. Petrol.* **53**, 875–890 (2012).
2. Wong, K. *et al.* Focused Mid-Crustal Magma Intrusion During Continental Break-Up in Ethiopia. *Geophys. Res. Lett.* **50**, e2023GL103257 (2023).
3. Iddon, F. & Edmonds, M. Volatile-Rich Magmas Distributed Through the Upper Crust in the Main Ethiopian Rift. *Geochem. Geophys. Geosystems* **21**, e2019-GC008904 (2020).
4. Rooney, T. O., Furman, T., Yirgu, G. & Ayalew, D. Structure of the Ethiopian lithosphere: Xenolith evidence in the Main Ethiopian Rift. *Geochim. Cosmochim. Acta* **69**, 3889–3910 (2005).
5. Gleeson, M. L. M. *et al.* Constraining magma storage conditions at a restless volcano in the Main Ethiopian Rift using phase equilibria models. *J. Volcanol. Geotherm. Res.* **337**, 44–61 (2017).